A nucleus-encoded chloroplast protein regulated by iron availability governs expression of the photosystem I subunit PsaA in Chlamydomonas reinhardtii

Legendre Lefebvre, Linnka; Choquet, Yves Marcel; Kuras, Richard; Loubery, Sylvain Philippe; Douchi, Damien; Goldschmidt-Clermont, Michel P.

How to cite

LEGENDRE LEFEBVRE, Linnka et al. A nucleus-encoded chloroplast protein regulated by iron availability governs expression of the photosystem I subunit PsaA in Chlamydomonas reinhardtii. In: Plant physiology, 2015, vol. 167, n° 4, p. 1527–1540. doi: 10.1104/pp.114.253906

This publication URL: https://archive-ouverte.unige.ch/unige:86435

Publication DOI: 10.1104/pp.114.253906

Running head:

Anterograde control of *psaA* expression

Corresponding author:

Michel Goldschmidt-Clermont

Department of Botany and Plant Biology

University of Geneva,

30 quai Ernest Ansermet,

1211 Geneva 4,

Switzerland

email: michel.goldschmidt-clermont@unige.ch

phone: +41 22 3796188

Research areas:

Membranes, Transport and Bioenergenetics

Signaling and Response

A nucleus-encoded helical-repeat protein which is regulated by iron availability controls chloroplast *psaA* mRNA expression in Chlamydomonas

Linnka Lefebvre-Legendre[1], Yves Choquet[2], Richard Kuras[2], Sylvain Loubéry[1], Damien Douchi[1] and Michel Goldschmidt-Clermont[1].

One-sentence summary:

A nucleus-encoded chloroplast protein, which is required for the stability and translation of *psaA* mRNA, is post-transcriptionally regulated in response to iron deprivation in Chlamydomonas.

Adresses:

[1] Department of Botany and Plant Biology and Department of Molecular Biology, University of Geneva, 30 quai Ernest Ansermet, 1211 Geneva 4, Switzerland

[2.] Unité Mixte de Recherche 7141, CNRS/Université Pierre et Marie Curie, Institut de Biologie Physico-Chimique, 13 rue Pierre et Marie Curie, 75005 Paris, France

Footnotes:

Financial sources:

This work was supported by the University of Geneva, the Swiss National Fund (grants 31003A_146300 and 3100A0-117712), the European Union's Seventh Framework Programme for Research, Technological Development and Demonstration (FP7 KBBE 2009-3 Sunbiopath, GA 245070), the French Centre National de la Recherche Scientifique and the Université Pierre et Marie Curie, Paris 06.

Corresponding author:

Michel Goldschmidt-Clermont

email: michel.goldschmidt-clermont@unige.ch

phone: +41 22 3796188

ABSTRACT

The biogenesis of the photosynthetic electron transfer chain in the thylakoid membranes requires the concerted expression of genes in the chloroplast and the nucleus. Chloroplast gene expression is subjected to anterograde control by a battery of nucleus-encoded proteins that are imported in the chloroplast where they mostly intervene at post-transcriptional steps. Using a new genetic screen, we identify a nuclear mutant which is required for expression of the PsaA subunit of Photosystem I in the chloroplast of *Chlamydomonas reinhardtii*. This mutant is affected in the stability and translation of *psaA* mRNA. The corresponding gene, named *TAA1* (translation of *psaA*), encodes a large protein with an array of octatrico-peptide repeats (OPR) and a RAP domain, both of which are thought to mediate RNA-binding. We show that as expected for its function, TAA1 is localized in the chloroplast. It was previously shown that when mixotrophic cultures of Chlamydomonas (which use both photosynthesis and mitochondrial respiration for growth) are shifted to conditions of iron limitation, there is a strong decrease in the accumulation of Photosystem I and that this is rapidly reversed when iron is re-supplied. Under these conditions, TAA1 protein is also down-regulated through a post-transcriptional mechanism, and rapidly re-accumulates when iron is restored. These observations reveal a concerted regulation of Photosystem I and of TAA1 in response to iron availability.

INTRODUCTION

Photosystem I (PSI) is a remarkable biological nano-device capable of using light energy to drive electron transfer reactions with a quantum yield that is close to 100 % (Amunts and Nelson, 2009). The core complex of PSI comprises 12 - 19 polypeptides (depending on the organism) that assemble together with up to two hundred cofactors that include chlorophylls, carotenoids, iron-sulfur clusters and phylloquinones. Some subunits are encoded in the chloroplast genome, while others are encoded in the nuclear genome and imported into the chloroplast. The biogenesis of PSI thus requires a tight coordination of gene expression in the nucleus and the chloroplast.

In *Chlamydomonas reinhardtii*, the core complex of PSI is composed of four chloroplast-encoded polypeptides, the two large subunits PsaA and PsaB and two smaller subunits, PsaC and PsaJ. The complex further comprises ten nuclear-encoded subunits. The coordinated biogenesis of PSI also marshals numerous nuclear genes that intervene in post-transcriptional steps of chloroplast gene expression and in the assembly of the complex. The *psaA* gene is split in three separate exons scattered in distant loci of the chloroplast genome (Kück et al., 1987). The exons are transcribed separately and the three precursors are assembled with the short *tscA* RNA to form the structures of two split introns of group II (Goldschmidt-Clermont et al., 1991). The introns are removed in two steps of *trans*-splicing to form the mature *psaA* mRNA (Choquet et al., 1988) . Genetic analysis of PSI-deficient Chlamydomonas mutants has revealed that at least fourteen nuclear loci are required for *trans*-splicing of *psaA* (Goldschmidt-Clermont et al., 1990). To date, six of the genetically-defined factors have been characterized in more detail. The processing of *tscA* from a polycistronic precursor requires RAA1, RAT1, RAT2 and RAA4. RAA1 is also required for the *trans*-splicing of both the introns (Hahn et al. 1998; Balczun et al. 2005; Merendino et al. 2006; Glanz et al. 2012). RAA3 is involved in *trans*-splicing of the first intron while RAA2 is required for *trans*-splicing of the second intron (Rivier et al. 2001; Perron et al. 1999, 2004). Biochemical studies have revealed several other proteins that bind to the *psaA* introns (Balczun et al., 2006; Glanz et al., 2006; Jacobs et al., 2013).

The assembly of PSI is assisted by two chloroplast-encoded proteins, Ycf3 and Ycf4, which are required at early steps in the formation of the functional complex (Boudreau et al., 2000; Naver et al., 2001; Onishi and Takahashi, 2009; Ozawa et al., 2009). The assembly begins with PsaB, which is produced under the control of TAB1 and TAB2. These nucleus-encoded proteins are necessary for translation initiation of *psaB* mRNA (Stampacchia et al., 1997; Dauvillee et al., 2003; Rahire et al., 2012). The synthesis of stoichiometric proportions of two other chloroplast-encoded polypeptides, PsaA and PsaC, is ensured through Control by Epistasy of Synthesis (CES): unassembled PsaA or PsaC

subunits exert negative feedback regulation on the translation of their respective mRNAs when they are produced in excess of PsaB (Wostrikoff et al., 2004). The stability of *psaC* mRNA depends on a newly discovered nucleus-encoded factor, Mac1 (Damien Douchi and MGC, unpublished). As described above, trans-splicing of *psaA* requires at least fourteen nucleus-encoded proteins. However *psaA trans*-splicing can be by-passed, without any apparent phenotypic consequence, by introducing an intron-less copy of the gene in the chloroplast genome (Lefebvre-Legendre et al., 2014). This suggests that the complex *trans*-splicing pathway does not play a predominant role in the regulation of PSI assembly, at least under a number of different growth conditions that were investigated. By analogy with *psaB* and *psaC*, and also with numerous subunits of the other photosynthetic complexes, it could be expected that other specific nucleus-encoded factors control the stability and translation of *psaA* mRNA. Genetic screens to identify such factors have been hindered by the large number of genetic loci which are required for *psaA trans*-splicing and constitute the prevalent mutational target. Here we present a genetic screen designed to identify amongst a collection of PSI mutants, those that would affect expression of *psaA* at a step other than *trans*-splicing. This led to the identification of TAA1, a nucleus-encoded factor required for the stability and translation of *psaA* mRNA. TAA1 turns over rapidly, and its levels are down-regulated under conditions of iron limitation.

RESULTS

Isolation of the *taa1* mutant

The *taa1* mutant (*translation of psaA*) was obtained by screening a collection of PSI-deficient mutants (Girard et al., 1980) to identify those whose genetic target is the 5' UTR of *psaA*. For this screen, the PSI mutants were transformed with two different plasmids bearing *aadA* chimeric genes which confer resistance to spectinomycin (Goldschmidt-Clermont, 1991). The tester construct *psaA-aadA* contained the *psaA* promoter and 5'UTR fused to *aadA* (Wostrikoff et al., 2004), while the positive control *atpA-aadA* contained the promoter and 5'UTR of *atpA* fused to *aadA*(Kuras et al., 1997). Transformation of the *taa1* mutant (formerly F23) with *psaA-aadA* failed to confer spectinomycin resistance while the control transformation with *atpA-aadA* allowed growth on the antibiotic, indicating that the promoter or 5'UTR of *psaA* is a target of TAA1.

To confirm this conclusion, the *taa1;mt(-)* mutant was crossed to a transformed strain carrying the *psaA-aadA* cassette (Wostrikoff et al., 2004). Due to the uniparental inheritance of the chloroplast genome, all the progeny received the *psaA-aadA* transgene from the mt(+) parent whereas only half of the progeny inherited the *taa1* mutation from the nuclear genome of the mt(-) parent. In 8 complete tetrads, all the PSI-deficient *taa1* progeny were unable to grow on

spectinomycin, while all the wild-type progeny did show resistance. This is illustrated with the four progeny of a representative tetrad: J11, J12, J13 and J14 (Figure 1A). In this tetrad, J13 and J14 had the wild-type TAA1 gene, as deduced from the presence of PsaA (Fig 1B) and their growth on minimal medium, while J11 and J12 carried the *taa1* mutation. The absence of TAA1 in J11 and J12 leads to a growth defect on photosynthetic medium and on spectinomycin plates. The results thus confirm that the promoter or 5'UTR of *psaA* is a target of TAA1. We noted that J14 grew more slowly, suggesting the presence of another mutation in the background of this strain. Therefore for the further analysis of taa1, the strain was backcrossed three times to the wild type. As shown by immuno-blot analysis, the amount of PsaA protein was reduced below detection levels in the *taa1* progeny, but present in the wild-type progeny (Figure 1B). There was a concomitant decrease in the level of the chimeric *psaA-aadA* mRNAs in the *taa1* progeny, J11 and J12, compared to the WT progeny J13 and J14 (Figure 1C). These data indicate that the absence of TAA1 leads to a defect in either the transcription or the accumulation of the chimeric *psaA* transcript, and an even stronger effect on the levels of the PsaA protein.

Identification of the *TAA1* gene

Transformation of the *taa1* mutant strain with an ordered cosmid library of genomic DNA allowed the identification of a cosmid (64B4) that could rescue photoautotrophic growth (Zhang et al., 1994). The 9.4 kb EcoRI subfragment of this cosmid (64B4E) was also able to rescue the *taa1* mutant (Supplementary Table 1). A BLAST search of the Chlamydomonas genome with the sequence of this subfragment identified a genomic region containing only one gene, Cre06.g262650 (Phytozome v9.1). The gene comprises 12 exons according to the assembly of EST data and the gene model predictions (Fig 2A). A partial cDNA (3.5kb) was isolated from a Chlamydomonas cDNA library using as hybridization probe a PCR fragment located in the 3'UTR of the gene. This cDNA corresponds to the last six exons, and its sequence is in accordance with the annotation of the transcript (Phytozome v9.1). Sequencing of RT-PCR fragments from the same region also confirmed the nucleotide sequence. The presence of three in-frame stop codons within 35 bp upstream of the translation initiation codon indicates that the complete coding sequence was identified. The deduced *TAA1* open reading frame encodes a protein of 2083 amino acid (207 kDa), which contains 7 tandem degenerate repeats of 38-40 amino acids belonging to the OPR family (Octotrico Peptide Repeat) (Auchincloss et al., 2002; Merendino et al., 2006; Eberhard et al., 2011; Rahire et al., 2012). The predicted polypeptide (Figure 2A and Supplementary Figure 1) shows a group of five OPR repeats (residues 928 to 1117), separated from two further repeats (residues 1448-1525), and a RAP domain (RNA-binding domain abundant in apicomplexans; residues 1978-2031). The OPR repeats are postulated to form α-helical RNA-binding domains and are also present in other Chlamydomonas

chloroplast proteins involved in post-transcriptional steps of mRNA expression (Auchincloss et al., 2002; Balczun et al., 2005; Merendino et al., 2006; Eberhard et al., 2011; Rahire et al., 2012). The RAP domain is thought to be an RNA-binding domain (Lee and Hong, 2004) and is also found in RAA3 which is involved in *trans*-splicing of *psaA* in Chlamydomonas (Rivier et al., 2001). When a stop codon was introduced in the TAA1 midigene upstream of the RAP domain (residue 1906), it lost its ability to rescue the *taa1* mutant, an indication that this domain may be functionally important (Supplementary Table 1). Altogether, these observations suggest that TAA1 could be involved in RNA metabolism.

A comparison of the cDNA sequences of the wild-type *TAA1* and of the *taa1* mutant, obtained by RT-PCR, revealed a single base substitution which changes Gln_{1327} to a stop codon (Figure 2A, marked with a star), located between the two OPR domains. The mapping of this mutation confirms that the *TAA1* gene was properly identified. Using a different genetic screen, Young and Purton (Young and Purton, 2014) identified several PSI-deficient mutants that could be rescued by transformation with *TAA1* genomic DNA (cosmid 64B4). In one of these mutants, allelism to *taa1* was confirmed by the presence of a mutation creating a stop codon in exon 5 of *TAA1*.

A *TAA1* "midigene" (pL30), was constructed as a fusion of a genomic fragment containing the 5' part of the gene (including 0.6kb upstream of the initiation codon and the first 6 introns) to the cDNA of the 3' part (Figure 2A; see Materials and Methods). Transformation of the *taa1* mutant with the midigene restored photoautotrophic growth (Figure 2B) at least as efficiently as the genomic fragment 64B4E (Supplementary Table 1). A rabbit polyclonal antibody was produced against a subfragment of TAA1 (amino acids 1335-1591). Using this TAA1 antiserum for immunoblotting, a weak band at 250 kDa was detected in protein extracts from the wild type that was absent in *taa1* (Figure 2C). This is significantly larger than the predicted mass of 207 kDa, but slow migration was previously observed for other Chlamydomonas proteins such as TAB1 (Rahire et al., 2012) or RAA1 (Merendino et al., 2006). This could be due to the presence of long hydrophobic stretches and the large size of these proteins. It is noteworthy that different levels of accumulation of TAA1 were observed in different wild-type laboratory strains of *C. reinhardtii*. Immunoblot analysis of total extracts from the *taa1* mutant transformed with the *TAA1* midigene (*taa1;cw15;TAA1*) revealed an over-expression of the TAA1 protein (Figure 2C). To facilitate the detection of TAA1, a version of the midigene carrying an HA epitope at the C-terminus was also constructed (Figure 2A and Materials and Methods). The mutant transformed with this construct, (*taa1;cw15;TAA1-HA)* grew photo-autotrophically on minimal medium, showing that the HA-tagged version of the *TAA1* midigene is functional (Figure 2B). This strain also over-expressed the TAA1 protein (Figure 2C). Northern-blot analysis showed no significant differences in the accumulation of the *psaA* mRNA in these strains

despite the over-expression of TAA1 (data not shown), and PsaA accumulated to normal levels (Fig 2C), suggesting that TAA1 is not limiting for *psaA* mRNA accumulation in the wild-type strain.

TAA1 is a chloroplast protein

To investigate the localization of the TAA1 protein, we took advantage of the *taa1;TAA1-HA* strain to facilitate its detection with the epitope tag. In a first approach, the subcellular distribution of TAA1 was investigated by confocal immunofluorescence microscopy. In order to validate the identification of different subcellular compartments, antibodies were used against either the PRK protein (Phospho Ribulo Kinase) which is located in the chloroplast (Figure 3A), or the 60S subunit of the cytoplasmic ribosome (Figure 3B). As a negative control for the HA immunofluorescence signal, the *taa1* mutant complemented with the similar midigene construct lacking the HA epitope tag (*taa1*;*TAA1*) was used. As expected (Figures 3A and 3B), no HA signal was detected in the latter strain. A co-localization of the TAA1-HA protein with the PRK protein was observed in the chloroplast, while the localization of TAA1 and the cytosolic 60S ribosome subunit were clearly distinct (Figure 3B). We used Van Steensel's analysis (for review see (Bolte and Cordelieres, 2006), to quantitatively confirm that the TAA1-HA and PRK signals were coincident (green curve in Fig. 3C), whereas the TAA1-HA and the ribosomal 60S subunit signals exhibited complementary patterns (blue curve in Fig. 3C). Accordingly, Manders' analysis showed that the overlap between the TAA1-HA and the PRK signals was 87±1.2% (average of Manders' coefficient on n=43 cells), whereas the overlap between the TAA1-HA signal and the cytosolic 60S ribosomal subunit was only 23±1.8% (n=53 cells; reviewed by (Bolte and Cordelieres, 2006)). These data indicate that TAA1 is a chloroplast protein, as predicted by the WolfpSort and PredAlgo algorithms (Horton et al., 2007; Tardif et al., 2012).

In a second experimental approach, the localization of TAA1 was monitored in cell fractionation experiments. Chloroplasts were prepared by Percoll gradient centrifugation. TAA1 was enriched in the chloroplast fraction, relative to the total cell extract. This enrichment paralleled the chloroplast proteins PsaA and PRK, whereas the cytosolic protein RPL37 was detectable only in the total extract (Figure 4). When isolated chloroplasts were further fractionated, TAA1 was found both in the crude membrane pellet together with PsaA and in the supernatant containing soluble proteins such as PRK. It should be noted that the non-specific bands detected by the anti-RPL37 and anti-PRK sera in the membrane pellet of the chloroplast (marked with a star in Fig. 3) do not correspond in size to RPL37 and PRK. The HA-tagged TAA1 protein is over-expressed in comparison to the native protein (Figure 2C) and since the majority is in the soluble fraction (Figure 3), it cannot be excluded that TAA1 is normally soluble but that its over-expression leads to its partial aggregation. Other chloroplast factors involved in RNA metabolism have also been detected in both soluble and membrane fractions

of the chloroplast (Boudreau et al., 2000; Vaistij et al., 2000; Rivier et al., 2001; Auchincloss et al., 2002).

The stability of *psaA* mRNA is impaired in the *taa1* mutant

To further characterize the *taa1* mutation, the mutant was back-crossed three times to the WT strain. The phenotypic analysis of the back-crossed strain confirmed the previous results: the absence of TAA1 leads to a defect in photo-autotrophic growth due to the absence of the PsaA protein (Figure 5A), and to a large decrease in *psaA* mRNA (Figure 5B). In order to determine whether the reduced accumulation of psaA mRNA in the absence of TAA1 is due to a defect in transcription or to increased degradation, the transcriptional activity of *psaA* was directly assessed in a run-on transcription assay (Klinbert et al. 2005). In this assay, RNA polymerases that were active on the gene at the time of cell lysis can further extend the nascent transcripts, but transcription initiation does not occur. Thus the amount of incorporation of radio-labelled nucleotides into specific transcripts reflects the loading of polymerases on the respective genes, and hence transcriptional activity. The radio-labelled RNA was hybridized to DNA probes; immobilized on a Nylon membrane; that included *psaA* exon 1 and *psaA* exon 3, as well as a five other chloroplast genes as positive controls and a bacterial plasmid as a negative control (pUC19). No difference in the transcriptional activity of *psaA* could be observed between the *taa1* mutant and the wild-type strain (Figure 5C). These results indicate that the absence of TAA1 does not lead to decreased transcription of the *psaA* gene. It can thus be inferred that lack of TAA1 leads to a specific decrease in the stability of the *psaA* mRNA.

TAA1 is required for translation of *psaA*

The stability of *psaA* transcripts is affected in *taa1* such that small amounts of mRNA are present, while the accumulation of PsaA protein is more strongly affected (Figure 5). This raises the question whether TAA1 is also involved in promoting the translation of *psaA* mRNA. It has been shown previously that some chloroplast transcripts are protected against 5’ to 3’ exo-nucleolytic degradation by RNA-binding proteins. In some of the corresponding nuclear mutants, stability of the target chloroplast RNA was restored by the insertion of a poly(G) cassette which can form a very stable secondary structure that impedes the progression of exoribonucleases (Drager et al., 1998; Drager et al., 1999; Nickelsen et al., 1999; Vaistij et al., 2000; Loiselay et al., 2008). In order to investigate the potential role of TAA1 in the protection and in the translation of *psaA*, a poly(G) tract was inserted by chloroplast transformation in the 5’UTR of *psaA* exon 1. The poly(G) tract was introduced in a transformation vector carrying an intron-less version of the *psaA* gene (*psaA-Δi*) (Lefebvre-Legendre et al. 2014). In this vector exons 1, 2 and 3 of *psaA* were fused and placed under the control of the *psaA*-exon 1 promoter and 5’UTR to bypass *trans*-splicing. The flanking sequences

in the vector were chosen such that after chloroplast transformation and homologous recombination, the intron-less gene replaces the resident *psaA*-exon3. In this construct (*pG-psaA-Δi*), 18 G residues were inserted in the 5'UTR of *psaA* at position 38 from the 5'end of the mRNA (-91 relative to the initiation codon). Biolistic transformants of *taa1* were selected on spectinomycin-containing medium and subcultured until homoplasmy was achieved (Supplementary Figure 2), giving strain *taa1/pG-psaA-Δi*. In order to create a nearly isogenic strain with the wild-type *TAA1* gene, the *taa1/pG-psaA-Δi* strain was rescued by nuclear transformation with the wild-type genomic DNA (cosmid 64B4E) to obtain the strain *taa1;TAA1/pG-psaA-Δi*, which was as expected capable of photo-autotrophic growth. Another control strain, *taa1/psaA-Δi*, containing the intron-less *psaA* gene without the poly(G) tract, was obtained by crossing the *taa1* mutant with the wild-type strain WT/*psaA-Δi* (Lefebvre-Legendre et al. 2014). The level of *psaA* mRNA in the different strains was determined by quantitative RT-PCR (Figure 6A), and the accumulation of *psaA* mRNA in the rescued strain, *taa1;TAA1/pG-psaA-Δi*, was set to 100%. As expected, the level of *psaA* was barely detectable in the *taa1* mutant, and was similarly low in the *taa1/psaA-Δi* strain, showing that the absence of introns in the *psaA* transcripts does not restore *psaA* mRNA accumulation. In contrast, *psaA* RNA carrying the poly(G) did accumulate in the *taa1* mutant background (*taa1/pG-psaA-Δi*) to 70% of the levels in the rescued control strain. These results provide evidence that TAA1 protects the *psaA* mRNA against 5' to 3' degradation (Figure 6C).

A further role of TAA1 in the translation of the *psaA* mRNA was investigated by determining the level of PsaA protein in the same strains (Figure 6B). As expected, we could not detect any PsaA in the *taa1* and *taa1/psaA-Δi* strains, while the protein was present in the rescued strain (*taa1-TAA1/pG-psaA-Δi)*. The normal accumulation of PsaA in the latter strain shows that the poly(G) tract does not interfere with translation. Interestingly, the PsaA protein was undetectable in the *taa1/pG-psaA-Δi* strain even though a nearly wild-type level of the *psaA* transcript was present (Figure 6A). These data strongly suggest that TAA1 is required for *psaA* translation in addition to its role in the stability of the *psaA* transcript (Figure 6C). This could be a direct role in promoting translation initiation, or an indirect role by ensuring the stability of sequences in the 5'UTR that would contain the binding site of another unidentified translation factor.

The role of TAA1 in RNA stability and translation suggested that it might associate with other factors and with the *psaA* mRNA. To investigate this possibility, an extract of *taa1;cw15;TAA1-HA* was fractionated by centrifugation in a sucrose gradient, and the fractions were analyzed by immunoblotting (Supplemental Figure 2). TAA1-HA sedimented with an apparent mass of 270 kDa, while when the sample was treated with RNase prior to fractionation, TAA-HA sedimented with an apparent mass of 200 kDa. Mock treatment without added RNase gave a similar shift, probably

because of endogenous RNase activity in the extract. Since the molecular mass of TAA1 is approximately 200 kDa, these data could suggest that TAA1 associates with RNA but is not part of a large multimolecular complex, unlike other Chlamydomonas chloroplast proteins of similar function (Vaistij et al., 2000; Boulouis et al., 2011).

Regulation of TAA1 in response to iron limitation.

It has been shown previously that Photosystem I is a prime target of protein degradation under iron deficiency in mixotrophic conditions, probably because of its high iron content (Moseley et al., 2002). Thus we investigated the behavior of TAA1 in response to iron limitation in three different Chlamydomonas lines (Figure 7). In our standard wild-type strain WT-8B, the analysis of TAA1 was hampered by a band that was detected in immunoblots migrating just ahead of TAA1 (Fig 7A; labeled with an asterisk). However this band was not detected in another wild-type strain, 137AH, or in the HA-tagged strain *taa1;TAA1::HA;cw15*. The comparison of the three strains indicates that the lower band of the doublet labelled by the anti-TAA1 serum in WT-8B is non-specific. Cells from cultures in exponential phase were harvested and resuspended in TAP lacking iron (TAP-Fe), and the cultures were further diluted after 24h and 48h to maintain a low cell density and exponential growth (Busch et al., 2008). After 48h, Fe^{2+} was supplemented to the normal concentration of 18 µM. Samples were collected at the onset of the experiment (labelled +Fe), after 24h and 48h of iron deprivation (labelled -Fe 24h and -Fe 48h) and after 24h of recovery (labelled +Fe 24h). In these conditions (Figure 7A), a large decrease in the level of the PsaA protein was observed after 48h of iron limitation whereas the accumulation of the ATP synthase (CF_1) remained unaltered, as previously observed (Moseley et al., 2002). A large reduction of TAA1 protein amounts was also observed under iron deficiency, a decrease that was already apparent after 24h. Following the re-supplementation of iron for 24h, both TAA1 and PsaA recovered to normal levels. These data indicate that there is a coordinate decrease of the TAA1 and PsaA proteins under iron limitation, and that the loss of TAA1 occurs earlier and is more extensive than that of PsaA.

To further elucidate this process, the RNA levels of *TAA1* and *psaA* were monitored by quantitative RT-PCR in the wild-type strain WT-8B. The amount of *psaA* mRNA was reduced already after 24h of iron deprivation (Figure 7B) and declined approximately 2-3 fold after 48h. The levels of the *TAA1* RNA remained essentially constant during iron limitation. Thus, the decrease in the level of the TAA1 protein cannot be attributed to reduced accumulation of the mRNA, but rather to a post-transcriptional process. A moderate increase in the level of *TAA1* mRNA was observed after iron re-

supplementation, but a concomitant increase in the level of TAA1 protein was only observed in one of the three strains examined (Figure 7A).

In order to better understand the post-transcriptional control of TAA1, we further investigated the fate of the TAA1 protein. To facilitate the detection of low levels of TAA1, the HA-tagged midigene strain *taa1;TAA1-HA;cw15* was used, where TAA1-HA can be detected with the anti-HA monoclonal antibody. As shown above, under iron limitation TAA1 and TAA1-HA respond in a similar way (Fig 7A). During iron deprivation, the protein levels were examined at an earlier time point (6 hours) in order to confirm whether the decrease of TAA1 occurs before the loss of PsaA, as was suggested by the previous experiments (Figures 7A). After 6 hours of iron starvation (6h –Fe), the level of TAA1 protein was already strongly decreased (approximately 4-fold; Fig. 7C, lane 7 versus lane 5), while PsaA only diminished after more than 24 hours (Figure 7A). To investigate the degradation of TAA1, aliquots of the cultures were supplemented with cycloheximide, an inhibitor of cytosolic translation. The treatment was initiated 2 hours after the beginning of iron starvation. In parallel, a control experiment was performed in the presence of normal levels of iron. Interestingly, in the presence of iron the content of TAA1 strongly decreased after addition of cycloheximide (approximately 10-fold in 6 hours), indicating that TAA1 protein is rapidly degraded under normal conditions (Figure 7C, lane 6 versus lane 5). In the absence of iron, TAA1 was degraded to even lower levels in the presence of cycloheximide (Figure 7C, lane 8 versus lane 6). These data suggest that TAA1 always has a constitutively short half-life and that under iron deficiency, its high rate of degradation is no longer counterbalanced by a matching rate of translation.

DISCUSSION

TAA1 is involved in *psaA* mRNA stability and translation

Photosynthetic protein complexes have a dual genetic origin, with some subunits encoded in the chloroplast and others in the nucleus. Therefore a concerted control of gene expression in the two compartments is necessary for the biogenesis of the thylakoid membrane. Coordinated accumulation of the different subunits involves several mechanisms. One of these is the proteolytic degradation of subunits that are not assembled into the photosynthetic complexes. In another mechanism, known as CES (Control by Epistasy of Synthesis), unassembled subunits induce negative feedback regulation of their own translation (Choquet and Wollman, 2009). Furthermore retrograde signals from the chloroplast to the nucleus control transcription of photosynthesis-related genes (Eberhard et al., 2008). Conversely the nucleus exerts tight anterograde control on expression of

organelle genes. In Chlamydomonas, the expression of chloroplast proteins is generally not limited by transcription, since rates of chloroplast translation are not very sensitive to changes in DNA or transcript levels (Eberhard et al., 2002). Anterograde control mainly occurs at post-transcriptional steps, mediated by nucleus-encoded factors that govern the expression of specific chloroplast genes. Some factors are involved in the stable accumulation of their cognate target transcripts (dubbed M factors, for maturation/stability) while others are primarily required for the translation of specific mRNAs (T factors) (Choquet and Wollman, 2002). For example in Chlamydomonas, MCA1 (Maturation of *petA*) protects the *petA* transcripts from 5' to 3' exonucleolytic degradation whereas TCA1 (Translation of *petA*) is primarily necessary for the translation of the *petA* mRNA (Wostrikoff et al., 2001; Raynaud et al., 2007; Loiselay et al., 2008). Likewise NAC2 is required for the stable accumulation of *psbD* mRNA while RB40 plays a role in its translation (Kuchka et al., 1989; Schwarz et al., 2007). In these two cases where both M and T factors for a specific transcript have been identified, they are found associated in a high molecular weight complex. In fact it has been shown that the mRNA-stability M-factor MCA1 is also necessary for the translation of the *petA* mRNA and that conversely in the absence of the translation T-factor TCA1, the level of *petA* mRNA is decreased (Loiselay et al., 2008; Boulouis et al., 2011). These examples illustrate the coupling of RNA stabilization and translation initiation in the Chlamydomonas chloroplast. Similarly, TAA1 may also act both as M- and T-factor: it is required for the stability of *psaA* mRNA but is also necessary for its translation. It cannot however be excluded that either of these roles could be indirect. That the target of TAA1 is in the 5'UTR of *psaA* suggests that its role of TAA1 in translation is exerted at the initiation step.

Because TAA1 is required for *psaA* RNA stability and translation, it is relevant that it contains two sequence features that are ascribed to RNA-binding activity: seven OPRs (octotricopeptide repeats) and a RAP domain (for RNA-binding domain abundant in Apicomplexans). This suggests that TAA1 may have a direct physical interaction with its RNA target in the 5'UTR of *psaA*. The OPR proteins belong to the super-family of helical-repeat proteins that also include the PPR (pentatrico peptide repeat), HAT (half a tetratricopeptide repeat) and mTERF proteins (mitochondrial termination factor) (reviewed by (Hammani et al., 2014)). Structural studies for some of these proteins have shown that the repeats form superhelical structures made of tandem antiparallel α-helices and it is believed that all these proteins have the same kind of structural organization. The best characterized are the PPR proteins of land plants which constitute a family of more than 400 members required for chloroplast or mitochondrial RNA metabolism including translation, RNA processing and RNA editing (Barkan and Small, 2014). Each PPR motif interacts with one base of the RNA target through a few amino-acid residues that mediate sequence-specific recognition (reviewed

by (Barkan and Small, 2014)). Chlamydomonas has only 10 PPR proteins (Tourasse et al., 2013) but harbors a large number of OPR proteins: 44 were initially identified but there are probably many more (Eberhard et al., 2011; Rahire et al., 2012; Hammani et al., 2014) (Olivier Vallon, personal communication). The OPR motif comprises 38 to 40 amino acids and is repeated between 2 and 24 times per protein. To date, 5 OPR proteins have been functionally characterized in Chlamydomonas. RAT2 and RAA1 are required for *trans*-splicing of the *psaA* transcripts (Balczun et al., 2005; Merendino et al., 2006), while TBC2, TAB1 and TDA1 are involved in the translation of *psbC*, *psaB* and *atpA* respectively (Auchincloss et al., 2002; Eberhard et al., 2011; Rahire et al., 2012).

In the *taa1* mutant, insertion of a polyG tract in the *psaA* 5'UTR compensated for the role of TAA1 in RNA stability (Figure 6). Using the same experimental approach, a function in protecting mRNA against 5'-3' exoribonucleases was demonstrated for other helical-repeat proteins in Chlamydomonas (Drager et al., 1998; Nickelsen et al., 1999; Vaistij et al., 2000; Loiselay et al., 2008). Likewise, the PPR10 protein of Arabidopsis was shown to protect its cognate RNAs *in vivo* and *in vitro* against exonucleolytic degradation from both directions (Pfalz et al., 2009; Prikryl et al., 2011). This is ascribed to the tight binding of the protein to the RNA, and leads to the accumulation of a characteristic small RNA footprint (Ruwe and Schmitz-Linneweber, 2012). Similarly in Chlamydomonas, the small RNAs protected by the HAT protein MBB1 coincide with the *cis*-acting elements required for RNA stability that were identified through chloroplast reverse genetics (Loizeau et al., 2014). An orthologue of MBB1 (HFC107) that also has the ability to yield small protected RNA footprints is conserved in maize and Arabidopsis (Hammani et al., 2012). A footprint reflecting the binding of TAA1 at the 5'end of the *psaA* mRNA was however not detected in the analysis of small chloroplast RNAs from Chlamydomonas (Loizeau et al., 2014).

Interestingly, TAA1 also contains a RAP domain that comprises approximately 60 amino acids and is predicted to be involved in diverse activities that involve RNA-binding (Lee and Hong, 2004). If TAA1 has a function both in RNA stability and in translation, the question arises whether one function is performed by the OPR motifs and the other by the RAP domain. However the single OPR protein present in Arabidopsis (RAP) shows a structure similar to TAA1 with 4 OPR repeats followed by a RAP domain and is specifically required for chloroplast 16S rRNA maturation (Kleinknecht et al., 2014) but is apparently not directly involved in translation.

A coordinate response to iron limitation

The restricted bio-availability of iron often limits photosynthesis in the oceans and on land. The electron transfer chains in the chloroplast and the mitochondrion are major sinks for iron. The abundance of other iron-dependent proteins may be comparatively small but they are essential for

fitness and stress acclimation (Page et al., 2012). Therefore, plants and algae optimize iron utilization in response to changes in its availability. In Chlamydomonas grown under iron limitation in mixotrophic conditions (i.e. photoheterotrophically in acetate-containing medium under the light), mitochondrial respiration is favored at the expense of photosynthesis (Moseley et al., 2002; Terauchi et al., 2010; Urzica et al., 2012). At the molecular level, photosystem I (PSI) degradation and the disconnection of its light-harvesting antenna are early targets of iron deficiency, presumably because of its high iron content (Moseley et al., 2002; Naumann et al., 2005). Under iron deficiency, iron that is released by PSI degradation is bound by ferritin, the translation of which is strongly and specifically induced (Busch et al., 2008). The acclimation response also involves other extensive changes in the composition of the transcriptome and of the proteome, in particular down-regulation of several transcripts that encode nucleus-encoded subunits of PSI and its antenna (Urzica et al., 2012; Hohner et al., 2013). While the acclimation response to iron limitation is largely manifested at the transcript level with matching changes in protein abundance, there are also a small set of proteins that are reduced in abundance while their mRNAs remain unaffected or increase, in particular Fe/S proteins (Urzica et al., 2012). Likewise, under iron limitation the TAA1 transcripts remain stable while the level of the protein strongly decreases, indicating that TAA1 is regulated post-transcriptionally . Even under normal iron-replete conditions, TAA1 has a short half-life. This is a characteristic of proteins that serve a regulatory function, allowing rapid changes in abundance through proteolytic degradation. Indeed the response of TAA1 to iron limitation is very fast, as a large decrease of the protein was observed already 6 hours after the transfer to iron-free medium.

A distinction can be made between anterograde control exerted by the nucleus on chloroplast gene expression through factors that are constitutively required, and anterograde regulation in a strict sense, where chloroplast gene expression is modified in response to environmental or developmental cues. During iron starvation the chloroplast-encoded PsaA subunit is down-regulated at the level of its mRNA and even more strongly at the level of protein accumulation. This correlates well with the concomitant decrease in TAA1 which exerts anterograde control on *psaA* mRNA stabilization and translation. It can thus be tentatively concluded that TAA1 is involved in regulating the synthesis of PsaA in response to iron availability. However it cannot be entirely ruled out that the acclimation response to iron starvation coordinately but separately regulates the expression of TAA1 and of PsaA.

An interesting parallel can be drawn with the regulation of the cytochrome b_6f complex under conditions of nitrogen limitation. This response involves the degradation of the b_6f complex, a reduction in the level of the corresponding chloroplast mRNAs, and a coordinated down-regulation of the proteins involved in b_6f biogenesis (Wei et al., 2014). The nucleus-encoded proteins MCA1 and

TCA1 are required for the stability and translation of *petA*, the chloroplast-encoded mRNA that encodes cytochrome f. MCA1 is also a short-lived protein that is rapidly degraded during nitrogen starvation (Raynaud et al., 2007) with a half-life (2 hrs) that is comparable to that of the TAA1 protein under iron deprivation (Figure 7).

The complexity of chloroplast RNA metabolism raises puzzling question on the evolution of chloroplast gene expression. A surprisingly numerous battery of nucleus-encoded factors intervene in the expression of specific plastid genes at post-transcriptional steps, such as processing, splicing, RNA stabilization, editing or translation (Stern et al., 2010; Barkan, 2011). Some of this complexity can be bypassed if introns or editing sites are removed from the chloroplast genome (Johanningmeier and Heiss, 1993; Minagawa and Crofts, 1994; Holloway et al., 1999; Schmitz-Linneweber et al., 2005; Petersen et al., 2011; Lefebvre-Legendre et al., 2014). In part the complexity may reflect a form of genetic drift, an evolutionary ratchet described by the theory of constructive neutral evolution (Gray et al., 2010). During evolution, some of the mutations that arise in the chloroplast genome could be compensated by the recruitment of nucleus-encoded RNA-binding factors capable of suppressing their phenotype, of "de-bugging" chloroplast gene expression (Maier et al., 2008), a mechanism we dub the "spoiled kid hypothesis" (Lefebvre-Legendre et al., 2014). However such mutations will only become fixed if they have a minimal fitness cost, implying that the suppressors must actually pre-exist the appearance of the mutations (Lynch, 2007; Gray et al., 2010). The large families of helical-repeat proteins with their modular architecture and simple mode of RNA recognition could contribute to a pool of such suppressors (Barkan and Small, 2014). However this futile aspect of complexity does not preclude that some of the nucleus-encoded proteins actually do play a role in anterograde regulation of chloroplast gene expression in response to developmental or environmental factors. The best studied examples are MCA1 and TCA1 and their role in the response to nitrogen supply. TAA1 and its response to iron availability may represent another actor in this type of regulation. Such regulatory activity could have been the function of these factors at early stages of their evolution, but alternatively they could have been co-opted for these regulatory roles from the complex pool of factors that had accumulated at later stages.

MATERIALS and METHODS

Strains and Media

The *Chlamydomonas reinhardtii* strains were grown in Tris-acetate-phosphate medium (TAP) or in high salt minimal medium (HSM) (Rochaix et al., 1988) to densities of 1–2 × 10^6 cells mL^{-1} in the dark or under fluorescent lights (60 µE m^{-2} s^{-1} or 6 µE m^{-2} s^{-1}) at 25 °C. For growth tests, 10 µl of cell culture at 2 × 10^6 cells mL^{-1} were spotted on agar plates and grown under 6 or 60 µE m^{-2} s^{-1} light as indicated. Where necessary, the TAP medium was supplemented with 100 µg mL^{-1} spectinomycin (Sigma Aldrich).

For growth under iron limitation, glassware was treated with 50 mM EDTA pH 8 and washed with milliQ water. TAP minus iron (TAP-Fe) was prepared with trace elements lacking Fe. For supplementation, Fe was added at 18 µM from a stock solution of 50 mM $FeSO_4$ chelated with 134 mM EDTA. For iron deprivation experiments, Chlamydomonas cells from cultures at 2 × 10^6 cells mL^{-1} were harvested by centrifugation and resuspended in TAP-Fe at 0.5 × 10^6 cells mL^{-1}. After 2h, Cycloheximide at 10 µg mL^{-1} and protease inhibitor cocktail (complete tablets EDTA-free from Roche) were added where indicated. After 24h and 48h, cells were diluted in TAP-Fe to 0.5 × 10^6 cells mL^{-1}. After the dilution at 48h, Fe was supplemented to 18 µM

Genetic analysis

For the genetic screen using chloroplast transformation of photosystem I deficient mutants (Girard et al., 1980), the tester construct *psaA-aadA* contained the *psaA-exon 1* promoter and 5'UTR fused to *aadA* (pfaAK(Wostrikoff et al., 2004)) and the positive control construct *atpA-aadA* contained the promoter and 5'UTR of *atpA* fused to *aadA* (pWFA; (Kuras et al., 1997)).

Crosses were performed using standard protocols (Harris, 1989). The *taa1* mutant was formerly named *F23* (Girard et al., 1980), it and was back-crossed 3 times to the wild-type. For nuclear transformation, the *taa1* mutant was crossed to the *cw15* strain to give *taa1;cw15*. The *F23* mutant was crossed to the strain *WT::aAK, mt+* (which carries a *psaA-aadA* marker; (Wostrikoff et al., 2004)). In 8 complete tetrads, the two PSI mutant progeny were unable to grow on 100 µg/mL spectinomycin while the two wild-type progeny grew like the *WT::aAK, mt+* parent. The strains J11, J12, J13 and J14 represent one of these tetrads. The *taa1* / *psaA-Δi* strain was obtained by crossing a WT/ *psaA-Δi* mt(+) strain with the *taa1;cw15* strain.

Nuclear transformations were achieved using the glass beads / vortex protocol (Kindle, 1990) and transformants were selected on HSM plates for photoautotrophic growth. Chloroplast

transformations were performed by Helium-gun bombardment and transformants were selected on TAP plates supplemented with 100 µg mL^{-1} spectinomycin, subcultured several times to obtain homoplasmic strains and genotyped by PCR (Supplementary Figure 2).

Cloning of the *TAA1* gene

By transformation of the *taa1* mutant (Shimogawara et al., 1998) with an ordered cosmid library and selection for photoautotrophic growth, the cosmid 64B4 was identified (Purton and Rochaix, 1994; Depege et al., 2003).This cosmid was digested with EcoRI, and a resulting 9.4 kb fragment, called 64B4E, was also capable of rescuing the *taa1* mutant.

The *TAA1* gene corresponds to Cre06.g262650 (Phytozome v10.0; http://phytozome.jgi.doe.gov/pz/portal.html#!info?alias=Org_Creinhardtii) and TAA1 is listed as OPR22 in (Rahire et al., 2012).

In order to identify the mutation in the *taa1* mutant, total RNA was extracted from the *taa1* and WT strains and subjected to RT-PCR (see below) using the following oligonucleotides : E9-down + 5103-up ; E9-up + E11-down; 3531-up + 4012-down; 4012-up + 5103-down. After agarose gel electrophoresis, the PCR fragments were purified and sequenced (Fasteris, Genève). Comparison of the mutant and WT products allowed the identification of a single base substitution which changes Gln_{1327} to a stop codon in the *taa1* mutant.

The cDNA clone #21 (exons 7-12) was isolated by screening a library constructed in bacteriophage lambda gt10 (Goldschmidt-Clermont and Rahire 1986), using a 0.6 kb PCR probe amplified with the oligonucleotides E11-down and 6541-up. The cDNA insert was excised with EcoRI and cloned into Bluescript KS (+) to give plasmid pL28. An EcoRI-XbaI fragment from cosmid 64B4, containing the 5'UTR and the beginning of the *TAA1* gene (0.66 kb upstream the ATG start codon and the first 5 kb of the *TAA1* gene), was cloned into Bluescript KS (+) to yield plasmid pL29. A 2.6 kb XbaI fragment of pL28 was inserted at the XbaI site of pL29 to give the midigene pL30.

The HA-tagged midigene, pL37, was constructed as follows. The oligonucleotides BspEI-For and Stop-rev and NsiI-Rev and Stop-For were used to generate by PCR using pL30 as the template, a modified 1.4 kb BspEI-NsiI fragment containing a StuI site just before the stop codon. This fragment was cloned into the pCR™II-TOPO® vector (Invitrogen) to yield plasmid pL33. A 1.5 kb EcoRV-BamHI fragment of pL33 was cloned into Bluescript KS (+) to give pL35. The StuI-NsiI fragment of pL35 was replaced by a synthetic StuI-NsiI fragment (Biomatik) containing a triple HA epitope fragment inserted between the StuI site and the stop codon, to yield plasmid pL36. Finally, the BspEI-NsiI fragment from pL30 was replaced by the BspEI-NsiI fragment of pL36, to provide the HA-tagged

midigene pL37. The TAA1 midigene carrying a C-terminal deletion lacking the RAP domain (pL57; stop codon at residue 1906) was obtained in two steps. Plasmid pL36 was digested with ZraI and StuI and religation to yield pL56. The BspEI-NsiI fragment of pL30 was then replaced by the corresponding fragment from pL56 to give pL57.

Insertion of a poly(G) cassette in the psaA 5' UTR

To introduce the poly(G) tract in the psaA 5' UTR, the AleI-XmaI fragment of psaA-Δi (pOS200) (Lefebvre-Legendre et al. 2014) was inserted into Bluescript KS (+) to give plasmid pL43. The NcoI-SphI fragment of pL43 containing the *psaA* 5' UTR was replaced by a synthetic NcoI-SphI fragment (Biomatik) where a tract of 18 G has been introduced 91 bp before the ATG translation initiation codon, to yield plasmid pL46. Finally, the modified AleI-XmaI fragment from pL46 was reintroduced into psaA-Δi (pOS200) to give plasmid pL47 (pG-psaA-Δi).

RT-PCR analysis of TAA1 transcripts

Total RNA was extracted from cells using RNeasy plant mini kit (Qiagen), total RNA were treated with DNase I (Qiagen) for 20 minutes at 25°C and repurified using the RNeasy mini kit (Qiagen). The RNA concentration was determined by spectrophotometry using a NanoDrop (Thermo Scientific) and the lack of genomic-DNA contamination or degradation was checked by gel electrophoresis. Reverse transcription was performed with 1 µg of total RNA using PrimeScript first-strand cDNA synthesis (Takara) following the manufacturer's instructions with random hexamer primers. For each experiment, a no-reverse transcription control was performed.

Quantitative PCR reactions were performed using LightCycler480 SYBR Green I Master (Roche) following the manufacturer's instructions. Water controls were included in each 96-well PCR plate, and dissociation analysis was performed at the end of each run to confirm the specificity of the reaction. The specificity of PCR products was checked by gel electrophoresis and DNA sequencing. Cycle threshold (Ct) values were obtained through LightCycler480 software release 1.5.0, and relative changes in gene expression were calculated using the $2^{-\Delta\Delta Ct}$ method using RPL13 for normalization. Experiments were performed in biological duplicates and technical triplicates. The following oligonucleotides (Supplementary Table 1) were used for the quantitative PCR reactions : for *psaA* exon1: qPCR-psaAEx1-For + qPCR-psaAEx3-Rev; for *TAA1*: qRT-TAA1-Fw1 + qRT-TAA1 Rv1; for *RPL13*: qRT-RPL13-For1 + qRT-RPL13-Rev1.

RNA analysis

Chlamydomonas cells from 50 mL cultures (2 × 10^6 cells mL^{-1}) were harvested by centrifugation and washed once with 10 mL of 20 mM Tris pH 7.9, and the pellets were stored at -70°C. For RNA extraction, 5 ml of Tri Reagent® (Sigma-Aldrich) and 500 µL of glass beads (G8772; Sigma-Aldrich) were added to the frozen pellets, and the suspensions were vigorously agitated for 2 min. The homogenates were split into 5 Phase Lock Gel™ tubes (5 PRIME, Hamburg, Germany). 400 µL of chloroform was added followed by thorough mixing. After 10 -min centrifugation at 14'000 g at 4 °C, 200 µL of chloroform was added followed by thorough mixing. After 10 -min centrifugation at 14'000 g at 4 °C, the RNA was precipitated from the aqueous phase with 1 mL isopropanol, collected by centrifugation and washed with 70% ethanol. Total RNA (5 µg) was analysed by formaldehyde agarose gel electrophoresis, transfer to Nylon membranes and hybridization using probes labelled with ^{32}P-dATP by random priming (Ausubel et al., 1998).

The chloroplast run-on transcription assay was performed as described (Klinkert et al., 2005).

Protein analysis

Chlamydomonas cells (5 mL, 2 × 10^6 cells mL^{-1}) were collected by centrifugation, washed with water, and resuspended in lysis buffer [100 mM Tris–HCl pH 6.8, 4% SDS, 20 mM EDTA, protease inhibitor cocktail (Sigma-Aldrich)]. After 30 min at room temperature, cell debris were removed by centrifugation, and total protein was analysed by SDS-PAGE (15%, 12% or 4% acrylamide) and immunoblotting. Labelling of the membranes with antisera against PsaA, D1, PRK, anti-cyt_f , RPL37 (Ramundo et al., 2013), anti-CF1 (gift of Sabeeha Merchant) or the monoclonal antibody HA-11 (Covance) was carried out at room temperature in 1× TBS (50 mM Tris–HCl pH 7.6, 150 mM NaCl), 0.1% Tween 20 and 5% w/v nonfat powder milk. After washing the membranes, the antibodies were revealed with a peroxidase-linked secondary antibody (Promega) and visualized by enhanced chemiluminescence.

Production of Polyclonal Antiserum of TAA1

The production of recombinant TAA1protein and generation of a polyclonal antiserum was performed as described by (Ramundo et al., 2013). The plasmid pL34, consisting of a fragment of *TAA1* (amino-acid residues 1335 to 1591) amplified with the oligonucleotides Ab-F23-2-For and Ab-F23-2-Rev, cloned between the BamHI and XhoI sites of vector pET28a (Novagen), was introduced into *Escherichia coli* BL21.

Cell fractionation

Cells were lyzed with a nebulizer and chloroplasts were purified on Percoll gradients as described previously (Rivier et al., 2001) in the presence of 0.1 mM of AEBSF. Chloroplasts were resuspended in hypotonic buffer [10 mM HEPES (pH 7.2), 5 mM $MgCl_2$, 1mM DTT] supplemented with protease inhibitor cocktail (Sigma-Aldrich). 250 µl of chloroplasts were lyzed by sonication, the solution was adjusted to 20 mM HEPES (pH 7.2), 50 mM KCl, 10 mM $MgCl_2$ and subjected to centrifugation at 100 000 g for 30 min at 4°C in a TLA45 rotor (Beckman). The supernatant was recovered for analysis, and the pellet was washed by resuspension in 20 mM HEPES (pH 7.2), 50 mM KCl, 10 mM $MgCl_2$, 0.2 M sucrose and centrifugation at 50 000 g for 15 min at 4°C in a TLA45 rotor. The supernatant was discarded and the pellet was resuspended in hypotonic buffer.

For sucrose gradient sedimentation analysis of TAA1, the cells from an exponential culture (2 10^6 cells mL^{-1}) were collected and resuspended at 5 10^8 cells mL^{-1} in 20 mM HEPES (pH 7.2), 50 mM KCl, 10 mM $MgCl_2$ plus protease inhibitors. Lysis was performed by freezing and thawing. The lysate was centrifuged for 20 min at 10,000 rpm at 4°C. One aliquot (1mL) of the supernatant was kept on ice, while two other aliquots were either supplemented with 100 µl of RNaseA (10 mg/ml in 100 mM Tris-HCl (pH 7.5) ,10 mM Na acetate) or with the same amount of buffer without RNase (mock treatment), followed by incubation at room temperature for 10 min. The samples (1 mL) were loaded on sucrose gradients (10 mL; 5-45% sucrose, 20 mM HEPES (pH 7.2), 50 mM KCl, 10 mM $MgCl_2$). After centrifugation at 173 000 g for 26h in the SW40 rotor (Beckman), 22 fractions (0.5 mL) were collected from the bottom by puncturing the tube. Sedimentation was calibrated with the Gel Filtration Calibration Kit HMW (SIGMA, GE28-4038-42).

Immuno-fluorescence microscopy

Slides were pretreated with a drop of a solution of 10% poly-lysine (Sigma) for 10 minutes and air-dried over-night. 1.5 × 10^6 cells were deposited and left to sediment and attach during 5 minutes. Fixation was done by incubating the slides for 5 minutes in a vertical slide holder filled with methanol pre-cooled to -20°C. After drying, the slides were incubated in blocking solution (PBST [137 mM NaCl, 2.7 mM KCl, 10 mM Na_2HPO_4, 2 mM KH_2PO_4, 0.1% v/v Tween 20], 1% w/v BSA, and 3% w/v fish skin gelatin) for 40 minutes, followed by 2 hours of incubation with a mix of 2 primary antisera (1:500 dilutions in blocking buffer), either rabbit anti-PRK with mouse monoclonal anti-HA-11 (Covance), or rabbit anti–60S with anti-HA-11. Anti-60S detects the ribosomal proteins of the 60S subunit of the cytoplasmic ribosome (Gift of W. Zerges, (Uniacke and Zerges, 2007)). After 3 washes of 10 minutes in PBST, cells were incubated for 2 hours in blocking buffer with secondary antibodies (goat anti-rabbit and goat anti-mouse antibodies coupled to Alexa488 or Alexa546 fluorophore

respectively (Life Technologies)). After 3 washes of 10 minutes in PBST, cells were finally washed one time in PBS and mounted in PBS + 50% glycerol.

Imaging was performed on an SP5 confocal laser scanning microscope (Leica) equipped with a resonant scanner and a 63x oil NA 1.4 PlanApo lens. The pinhole was opened at 1 Airy and the zoom was set so that the pixel size was comprised between 80nm and 120nm. Alexa488 and Alexa546 were imaged sequentially; they were respectively excited using the 488nm and 550nm lines of a white-light laser, and their fluorescence was recorded by two HyD detectors in the ranges of 500-550nm and 560nm-610nm, respectively. Maximum intensity projections were subsequently performed and displayed.

Image analysis was performed using ImageJ (W.S. Rasband, http://imagej.nih.gov/ij) and colocalization analysis was performed using the ImageJ JACoP plugin (Bolte and Cordelieres, 2006). Initially for each confocal stack and for each fluorescence channel the mean background signal was measured in a region outside of the cells, and subtracted from each z plane. Using the JACoP plugin (Bolte and Cordelieres, 2006), thresholds for the fluorescence signals were set manually, Manders' coefficients and Van Steensel's values were calculated on each z plane and then integrated over the whole z stack. Values obtained on different cells were finally averaged, and results are presented as mean ± standard error of the mean.

SUPPLEMENTAL DATA

Supplementary Figure 1. Structure of the TAA1 protein

Supplementary Figure 2. Sucrose gradient sedimentation analysis of TAA1 complexes.

Supplementary Figure 3. Genotyping of the *taa1/pG-psaA-Δi* chloroplast transformant

Supplementary Table 1. Rescue of *taa1* by transformation with *TAA1* constructs.

Supplementary Table 2. Oligonucleotides used in this work

ACKNOWLEDGEMENTS

We thank Dr. William Zerges for a gift of anti-60S antiserum and Drs Jean-David Rochaix and Francis-André Wollman for their scientific advice and comments on the manuscript.

LITERATURE CITED

Amunts A, Nelson N (2009) Plant photosystem I design in the light of evolution. Structure **17:** 637-650

Auchincloss AH, Zerges W, Perron K, Girard-Bascou J, Rochaix JD (2002) Characterization of Tbc2, a nucleus-encoded factor specifically required for translation of the chloroplast psbC mRNA in Chlamydomonas reinhardtii. J Cell Biol **157:** 953-962

Ausubel FA, Brent R, Kingston RE, Moore DD, Seidman JG, Smith JA, Struhl K (1998) Current Protocols in Molecular Biology. John Wiley & sons, New York, NY

Balczun C, Bunse A, Hahn D, Bennoun P, Nickelsen J, Kuck U (2005) Two adjacent nuclear genes are required for functional complementation of a chloroplast trans-splicing mutant from Chlamydomonas reinhardtii. Plant J **43:** 636-648

Balczun C, Bunse A, Schwarz C, Piotrowski M, Kuck U (2006) Chloroplast heat shock protein Cpn60 from Chlamydomonas reinhardtii exhibits a novel function as a group II intron-specific RNA-binding protein. FEBS Lett **580:** 4527-4532

Barkan A (2011) Expression of plastid genes: organelle-specific elaborations on a prokaryotic scaffold. Plant Physiol **155:** 1520-1532

Barkan A, Small I (2014) Pentatricopeptide Repeat Proteins in Plants. Annu Rev Plant Biol

Bolte S, Cordelieres FP (2006) A guided tour into subcellular colocalization analysis in light microscopy. J Microsc **224:** 213-232

Boudreau E, Nickelsen J, Lemaire SD, Ossenbuhl F, Rochaix JD (2000) The Nac2 gene of Chlamydomonas encodes a chloroplast TPR-like protein involved in psbD mRNA stability. Embo J **19:** 3366-3376

Boulouis A, Raynaud C, Bujaldon S, Aznar A, Wollman FA, Choquet Y (2011) The nucleus-encoded trans-acting factor MCA1 plays a critical role in the regulation of cytochrome f synthesis in Chlamydomonas chloroplasts. Plant Cell **23:** 333-349

Busch A, Rimbauld B, Naumann B, Rensch S, Hippler M (2008) Ferritin is required for rapid remodeling of the photosynthetic apparatus and minimizes photo-oxidative stress in response to iron availability in Chlamydomonas reinhardtii. Plant J **55:** 201-211

Choquet Y, Goldschmidt-Clermont M, Girard-Bascou J, Kuck U, Bennoun P, Rochaix JD (1988) Mutant phenotypes support a trans-splicing mechanism for the expression of the tripartite psaA gene in the C. reinhardtii chloroplast. Cell **52:** 903-913

Choquet Y, Wollman FA (2002) Translational regulations as specific traits of chloroplast gene expression. FEBS Lett **529:** 39-42

Choquet Y, Wollman FA (2009) The CES process. *In* D Stern, EH Harris, eds, The Chlamydomonas Sourcebook: Organellar and Metabolic Processes. Academic Press, Oxford, pp 1027-1064

Dauvillee D, Stampacchia O, Girard-Bascou J, Rochaix JD (2003) Tab2 is a novel conserved RNA binding protein required for translation of the chloroplast psaB mRNA. EMBO J **22:** 6378-6388

Depege N, Bellafiore S, Rochaix JD (2003) Role of chloroplast protein kinase Stt7 in LHCII phosphorylation and state transition in Chlamydomonas. Science **299:** 1572-1575

Drager RG, Girard-Bascou J, Choquet Y, Kindle KL, Stern DB (1998) In vivo evidence for 5'-->3' exoribonuclease degradation of an unstable chloroplast mRNA. Plant J **13:** 85-96

Drager RG, Higgs DC, Kindle KL, Stern DB (1999) 5' to 3' exoribonucleolytic activity is a normal component of chloroplast mRNA decay pathways. Plant J **19:** 521-531

Eberhard S, Drapier D, Wollman FA (2002) Searching limiting steps in the expression of chloroplast-encoded proteins: relations between gene copy number, transcription, transcript abundance and translation rate in the chloroplast of Chlamydomonas reinhardtii. Plant J **31:** 149-160

Eberhard S, Finazzi G, Wollman FA (2008) The dynamics of photosynthesis. Annual review of genetics **42:** 463-515

Eberhard S, Loiselay C, Drapier D, Bujaldon S, Girard-Bascou J, Kuras R, Choquet Y, Wollman FA (2011) Dual functions of the nucleus-encoded factor TDA1 in trapping and translation

activation of atpA transcripts in Chlamydomonas reinhardtii chloroplasts. Plant J **67:** 1055-1066

Girard J, Chua NH, Bennoun P, Schmidt G, Delosme M (1980) Studies on mutants deficient in the photosystem I reaction centers in Chlamydomonas reinhardtii. Curr Genet **2:** 215-221

Glanz S, Bunse A, Wimbert A, Balczun C, Kuck U (2006) A nucleosome assembly protein-like polypeptide binds to chloroplast group II intron RNA in Chlamydomonas reinhardtii. Nucleic Acids Res **34:** 5337-5351

Goldschmidt-Clermont M (1991) Transgenic expression of aminoglycoside adenine transferase in the chloroplast: a selectable marker of site-directed transformation of chlamydomonas. Nucleic Acids Res **19:** 4083-4089

Goldschmidt-Clermont M, Choquet Y, Girard-Bascou J, Michel F, Schirmer-Rahire M, Rochaix JD (1991) A small chloroplast RNA may be required for trans-splicing in Chlamydomonas reinhardtii. Cell **65:** 135-143

Goldschmidt-Clermont M, Girard-Bascou J, Choquet Y, Rochaix JD (1990) Trans-splicing mutants of Chlamydomonas reinhardtii. Mol Gen Genet **223:** 417-425

Gray MW, Lukes J, Archibald JM, Keeling PJ, Doolittle WF (2010) Cell biology. Irremediable complexity? Science **330:** 920-921

Hammani K, Bonnard G, Bouchoucha A, Gobert A, Pinker F, Salinas T, Giege P (2014) Helical repeats modular proteins are major players for organelle gene expression. Biochimie **100:** 141-150

Hammani K, Cook WB, Barkan A (2012) RNA binding and RNA remodeling activities of the half-a-tetratricopeptide (HAT) protein HCF107 underlie its effects on gene expression. Proc Natl Acad Sci U S A **109:** 5651-5656

Hohner R, Barth J, Magneschi L, Jaeger D, Niehues A, Bald T, Grossman A, Fufezan C, Hippler M (2013) The metabolic status drives acclimation of iron deficiency responses in Chlamydomonas reinhardtii as revealed by proteomics based hierarchical clustering and reverse genetics. Mol Cell Proteomics **12:** 2774-2790

Holloway SP, Deshpande NN, Herrin DL (1999) The catalytic group-I introns of the psbA gene of chlamydomonas reinhardtii : core structures, ORFs and evolutionary implications. Curr Genet **36:** 69-78

Horton P, Park KJ, Obayashi T, Fujita N, Harada H, Adams-Collier CJ, Nakai K (2007) WoLF PSORT: protein localization predictor. Nucleic Acids Res **35:** W585-587

Jacobs J, Marx C, Kock V, Reifschneider O, Franzel B, Krisp C, Wolters D, Kuck U (2013) Identification of a chloroplast ribonucleoprotein complex containing trans-splicing factors, intron RNA, and novel components. Mol Cell Proteomics **12:** 1912-1925

Johanningmeier U, Heiss S (1993) Construction of a Chlamydomonas reinhardtii mutant with an intronless psbA gene. Plant Mol Biol **22:** 91-99

Kindle KL (1990) High-frequency nuclear transformation of Chlamydomonas reinhardtii. Proc Natl Acad Sci U S A **87:** 1228-1232

Kleinknecht L, Wang F, Stube R, Philippar K, Nickelsen J, Bohne AV (2014) RAP, the sole octotricopeptide repeat protein in Arabidopsis, is required for chloroplast 16S rRNA maturation. Plant Cell **26:** 777-787

Klinkert B, Schwarz C, Pohlmann S, Pierre Y, Girard-Bascou J, Nickelsen J (2005) Relationship between mRNA levels and protein accumulation in a chloroplast promoter-mutant of Chlamydomonas reinhardtii. Mol Genet Genomics **274:** 637-643

Kuchka MR, Goldschmidt-Clermont M, van Dillewijn J, Rochaix JD (1989) Mutation at the Chlamydomonas nuclear NAC2 locus specifically affects stability of the chloroplast psbD transcript encoding polypeptide D2 of PS II. Cell **58:** 869-876

Kück U, Choquet Y, Schneider M, Dron M, Bennoun P (1987) Structural and transcription analysis of the two homolgous genes for the P700 chlorophyll a-apoprotein in Chlamydomonas reinhardtii: evidence for in vivo trans-splicing. Embo J **6:** 2185-2195

Kuras R, de Vitry C, Choquet Y, Girard-Bascou J, Culler D, Buschlen S, Merchant S, Wollman FA (1997) Molecular genetic identification of a pathway for heme binding to cytochrome b6. J Biol Chem **272:** 32427-32435

Lee I, Hong W (2004) RAP--a putative RNA-binding domain. Trends Biochem Sci **29:** 567-570

Lefebvre-Legendre L, Merendino L, Rivier C, Goldschmidt-Clermont M (2014) On the Complexity of Chloroplast RNA Metabolism: psaA Trans-splicing Can be Bypassed in Chlamydomonas. Mol Biol Evol **31:** 2697-2707

Loiselay C, Gumpel NJ, Girard-Bascou J, Watson AT, Purton S, Wollman FA, Choquet Y (2008) Molecular identification and function of cis- and trans-acting determinants for petA transcript stability in Chlamydomonas reinhardtii chloroplasts. Mol Cell Biol **28:** 5529-5542

Loizeau K, Qu Y, Depp S, Fiechter V, Ruwe H, Lefebvre-Legendre L, Schmitz-Linneweber C, Goldschmidt-Clermont M (2014) Small RNAs reveal two target sites of the RNA-maturation factor Mbb1 in the chloroplast of Chlamydomonas. Nucleic Acids Res **42:** 3286-3297

Lynch M (2007) The origins of genome architecture. Sinauer Associates, Inc., Sunderland, Mass., USA

Maier UG, Bozarth A, Funk HT, Zauner S, Rensing SA, Schmitz-Linneweber C, Borner T, Tillich M (2008) Complex chloroplast RNA metabolism: just debugging the genetic programme? BMC Biol **6:** 36

Merendino L, Perron K, Rahire M, Howald I, Rochaix JD, Goldschmidt-Clermont M (2006) A novel multifunctional factor involved in trans-splicing of chloroplast introns in Chlamydomonas. Nucleic Acids Res **34:** 262-274

Minagawa J, Crofts A (1994) A robust protocol for site-directed mutagenesis of the D1 protein in *Chlamydomonas reinhardtii*. Photosynth Res **42:** 121-131

Moseley JL, Allinger T, Herzog S, Hoerth P, Wehinger E, Merchant S, Hippler M (2002) Adaptation to Fe-deficiency requires remodeling of the photosynthetic apparatus. EMBO J **21:** 6709-6720

Naumann B, Stauber EJ, Busch A, Sommer F, Hippler M (2005) N-terminal processing of Lhca3 Is a key step in remodeling of the photosystem I-light-harvesting complex under iron deficiency in Chlamydomonas reinhardtii. J Biol Chem **280:** 20431-20441

Naver H, Boudreau E, Rochaix JD (2001) Functional studies of Ycf3: its role in assembly of photosystem I and interactions with some of its subunits. Plant Cell **13:** 2731-2745

Nickelsen J, Fleischmann M, Boudreau E, Rahire M, Rochaix JD (1999) Identification of cis-acting RNA leader elements required for chloroplast psbD gene expression in Chlamydomonas. Plant Cell **11:** 957-970

Onishi T, Takahashi Y (2009) Effects of site-directed mutations in the chloroplast-encoded Ycf4 gene on PSI complex assembly in the green alga Chlamydomonas reinhardtii. Plant Cell Physiol **50:** 1750-1760

Ozawa S, Nield J, Terao A, Stauber EJ, Hippler M, Koike H, Rochaix JD, Takahashi Y (2009) Biochemical and structural studies of the large Ycf4-photosystem I assembly complex of the green alga Chlamydomonas reinhardtii. Plant Cell **21:** 2424-2442

Page MD, Allen MD, Kropat J, Urzica EI, Karpowicz SJ, Hsieh SI, Loo JA, Merchant SS (2012) Fe sparing and Fe recycling contribute to increased superoxide dismutase capacity in iron-starved Chlamydomonas reinhardtii. Plant Cell **24:** 2649-2665

Petersen K, Schottler MA, Karcher D, Thiele W, Bock R (2011) Elimination of a group II intron from a plastid gene causes a mutant phenotype. Nucleic Acids Res **39:** 5181-5192

Pfalz J, Bayraktar OA, Prikryl J, Barkan A (2009) Site-specific binding of a PPR protein defines and stabilizes 5' and 3' mRNA termini in chloroplasts. EMBO J **28:** 2042-2052

Prikryl J, Rojas M, Schuster G, Barkan A (2011) Mechanism of RNA stabilization and translational activation by a pentatricopeptide repeat protein. Proc Natl Acad Sci U S A **108:** 415-420

Purton S, Rochaix JD (1994) Complementation of a Chlamydomonas reinhardtii mutant using a genomic cosmid library. Plant Mol Biol **24:** 533-537

Rahire M, Laroche F, Cerutti L, Rochaix JD (2012) Identification of an OPR protein involved in the translation initiation of the PsaB subunit of photosystem I. Plant J **72:** 652-661

Ramundo S, Rahire M, Schaad O, Rochaix JD (2013) Repression of essential chloroplast genes reveals new signaling pathways and regulatory feedback loops in chlamydomonas. Plant Cell **25:** 167-186

Raynaud C, Loiselay C, Wostrikoff K, Kuras R, Girard-Bascou J, Wollman FA, Choquet Y (2007) Evidence for regulatory function of nucleus-encoded factors on mRNA stabilization and translation in the chloroplast. Proc Natl Acad Sci U S A **104:** 9093-9098

Rivier C, Goldschmidt-Clermont M, Rochaix JD (2001) Identification of an RNA-protein complex involved in chloroplast group II intron trans-splicing in Chlamydomonas reinhardtii. Embo J **20:** 1765-1773

Ruwe H, Schmitz-Linneweber C (2012) Short non-coding RNA fragments accumulating in chloroplasts: footprints of RNA binding proteins? Nucleic Acids Res **40:** 3106-3116

Schmitz-Linneweber C, Kushnir S, Babiychuk E, Poltnigg P, Herrmann RG, Maier RM (2005) Pigment deficiency in nightshade/tobacco cybrids is caused by the failure to edit the plastid ATPase alpha-subunit mRNA. Plant Cell **17:** 1815-1828

Schwarz C, Elles I, Kortmann J, Piotrowski M, Nickelsen J (2007) Synthesis of the D2 protein of photosystem II in Chlamydomonas is controlled by a high molecular mass complex containing the RNA stabilization factor Nac2 and the translational activator RBP40. Plant Cell **19:** 3627-3639

Shimogawara K, Fujiwara S, Grossman A, Usuda H (1998) High-efficiency transformation of Chlamydomonas reinhardtii by electroporation. Genetics **148:** 1821-1828

Stampacchia O, Girard-Bascou J, Zanasco JL, Zerges W, Bennoun P, Rochaix JD (1997) A nuclear-encoded function essential for translation of the chloroplast psaB mRNA in chlamydomonas. Plant Cell **9:** 773-782

Stern DB, Goldschmidt-Clermont M, Hanson MR (2010) Chloroplast RNA metabolism. Annu Rev Plant Biol **61:** 125-155

Tardif M, Atteia A, Specht M, Cogne G, Rolland N, Brugiere S, Hippler M, Ferro M, Bruley C, Peltier G, Vallon O, Cournac L (2012) PredAlgo: a new subcellular localization prediction tool dedicated to green algae. Mol Biol Evol **29:** 3625-3639

Terauchi AM, Peers G, Kobayashi MC, Niyogi KK, Merchant SS (2010) Trophic status of Chlamydomonas reinhardtii influences the impact of iron deficiency on photosynthesis. Photosynthesis research **105:** 39-49

Tourasse NJ, Choquet Y, Vallon O (2013) PPR proteins of green algae. RNA Biol **10**

Uniacke J, Zerges W (2007) Photosystem II assembly and repair are differentially localized in Chlamydomonas. Plant Cell **19:** 3640-3654

Urzica EI, Casero D, Yamasaki H, Hsieh SI, Adler LN, Karpowicz SJ, Blaby-Haas CE, Clarke SG, Loo JA, Pellegrini M, Merchant SS (2012) Systems and trans-system level analysis identifies conserved iron deficiency responses in the plant lineage. Plant Cell **24:** 3921-3948

Vaistij FE, Boudreau E, Lemaire SD, Goldschmidt-Clermont M, Rochaix JD (2000) Characterization of Mbb1, a nucleus-encoded tetratricopeptide-like repeat protein required for expression of the chloroplast psbB/psbT/psbH gene cluster in Chlamydomonas reinhardtii. Proc Natl Acad Sci U S A **97:** 14813-14818

Vaistij FE, Goldschmidt-Clermont M, Wostrikoff K, Rochaix JD (2000) Stability determinants in the chloroplast psbB/T/H mRNAs of Chlamydomonas reinhardtii. Plant J **21:** 469-482

Wei L, Derrien B, Gautier A, Houille-Vernes L, Boulouis A, Saint-Marcoux D, Malnoe A, Rappaport F, de Vitry C, Vallon O, Choquet Y, Wollman FA (2014) Nitric Oxide-Triggered Remodeling of Chloroplast Bioenergetics and Thylakoid Proteins upon Nitrogen Starvation in Chlamydomonas reinhardtii. Plant Cell

Wostrikoff K, Choquet Y, Wollman FA, Girard-Bascou J (2001) TCA1, a single nuclear-encoded translational activator specific for petA mRNA in Chlamydomonas reinhardtii chloroplast. Genetics **159:** 119-132

Wostrikoff K, Girard-Bascou J, Wollman FA, Choquet Y (2004) Biogenesis of PSI involves a cascade of translational autoregulation in the chloroplast of Chlamydomonas. Embo J **23:** 2696-2705

Young RE, Purton S (2014) Cytosine deaminase as a negative selectable marker for the microalgal chloroplast: a strategy for the isolation of nuclear mutations that affect chloroplast gene expression. Plant J **80:** 915-925

Zhang H, Herman PL, Weeks DP (1994) Gene isolation through genomic complementation using an indexed library of Chlamydomonas reinhardtii DNA. Plant Mol Biol **24:** 663-672

FIGURE LEGENDS

Figure 1. The 5'UTR of *psaA* is a genetic target of *TAA1*

A. Spot tests

Chlamydomonas cultures were spotted (10 µL) on minimal medium (HSM), on medium containing acetate (TAP) or on TAP medium supplemented with 100 µg mL^{-1} spectinomycin (TAP+Spec) under normal light (60 µE m^{-2} s^{-1}). J11 to J14 are the progeny of a tetrad from the cross *psaA*::*aadA;mt(+)* x *taa1;mt(-)*. The *psaA*::*aadA;mt+* strain is a chloroplast transformant with the *aadA* gene (conferring resistance to spectinomycin) under the control of the promoter/5' UTR of *psaA*. Wild-type (WT) and *taa1* strains are shown as controls.

B. Immunoblot analysis of PsaA

Total protein extracts from the progeny of the same tetrad were subjected to SDS-PAGE and immunoblotting with anti-sera against PsaA or the D1 protein of photosystem II as a loading control. The algae were grown in medium containing acetate (TAP) in the dark.

C. RNA-blot analysis of *psaA* mRNA

Total RNA extracts from the progeny of the same tetrad were subjected to denaturing agarose gel electrophoresis, blotted to Nylon membranes and hybridized with probes against *aadA* or *atpB* as a control. The nature of the lower band which is routinely observed for *aadA* is not known (Goldschmidt-Clermont, 1991).

Figure 2. Characterization of the *TAA1* gene

A. Map of the *TAA1* gene

The first line is a schematic representation of the structure of the *TAA1* gene. The predicted pre-mRNA is 9'250 bp long, with a 5'UTR of 88 bp and a 3'UTR of 770 bp. The second line represents the structure of the midigene constructs with exons depicted as light grey boxes and the promoter / 5'UTR in dark gray. The 5' part of the genomic DNA is fused to the 3'part of the cDNA as shown with dotted lines. The flag represents the position of the triple HA epitope tag in pL37. The third line shows the exon structure of the coding sequence of *TAA1*. The bottom line depicts the structure of the TAA1 protein with the 7 OPR motifs shown as grey boxes and the RAP domain as hatched box. The star indicates the location of the premature stop codon in the *taa1* mutant.

B. Growth phenotype

Comparison of growth on minimal medium (HSM) and on medium containing acetate (TAP) under normal light (60 µE m^{-2} s^{-1}) of the mutant strain *taa1;cw15*, the control strain *cw15* and the complemented strains *taa1*;*cw15*;*TAA1* (transformed with the midigene pL30) and *taa1*;*cw15*;*TAA1-HA* (transformed with the midigene carrying a triple HA epitope, pL37).

C. Immunoblot analysis

Total protein extracts from the same strains were subjected to SDS-PAGE and immunoblotting with anti-sera against TAA1, PsaA, the CF_1 component of ATP synthase, and cytochrome f. The algae were grown in medium containing acetate (TAP) in the dark.

Figure 3. TAA1 is located in the chloroplast

A. Immuno-fluorescence of TAA1-HA in comparison to chloroplastic PRK

The first line represents staining in the *taa1* mutant strain complemented with the midigene carrying the triple HA epitope, *taa1*;*cw15*;*TAA1-HA*. The second line represents as a control the staining in the complemented strain with the midigene, *taa1*;*cw15*;*TAA1*.

B. Immuno-fluorescence staining pattern of the TAA1-HA protein in comparison to the cytosolic 60S ribosome subunit

The first line represents the staining in the *taa1*;*cw15*;*TAA1-HA* strain. The second line represents as a control the staining in the *taa1*;*cw15*;*TAA1* strain.

C. Quantitative analysis of co-localization

Van Steensel's analysis was applied to the co-stainings of TAA1-HA and PRK (green curves; average (thick line) ± standard error (thin lines) of n=43 cells) and of TAA1-HA and the ribosomal 60S subunit (blue curves; n=53 cells). This analysis consists in measuring Pearson's correlation coefficient between two fluorescent channels of a given image, and to plot the different values of this coefficient as one channel is shifted in x pixel by pixel relative to the other (see for review (Bolte and Cordelieres, 2006)). A peak at the δx=0 position indicates co-localisation of the two proteins studied (green curve: TAA1-HA and PRK); conversely, a local minimum at the δx=0 position indicates that the two signals are complementary (blue curve: TAA1-HA and the 60S ribosome subunit).

Figure 4. TAA1 is a partially soluble protein of the chloroplast

Fractions were prepared from the strain *taa1*;*cw15*;*TAA1-HA*. The four lanes contain total cell extracts (Total), the chloroplast fraction (Cp) and a chloroplast lysate fractionated by centrifugation into a soluble fraction (Supernatant) and a crude membrane fraction (Pellet). Equal amounts of protein (40µg) were loaded. Immunoblots were performed with antibodies against the HA epitope, PsaA (an integral membrane protein of Photosystem I), the cytosolic ribosomal protein RPL37 and PRK, a soluble chloroplastic protein. The bands marked with a star represent non-specific signals.

Figure 5. Stability of *psaA* mRNA is impaired in the *taa1* mutant

A. Immunoblot analysis of PsaA

Total protein extracts were subjected to SDS-PAGE and immunoblotting with anti-sera against PsaA and the D1 protein of photosystem II as a loading control. The algae were grown in medium containing acetate (TAP) in the dark.

B. RNA-blot analysis of *psaA* mRNA

Total RNA extracts from the same strains were subjected to denaturing agarose gel electrophoresis, blotted to Nylon membranes and hybridized with radiolabelled probes for exon 3 of *psaA*, or *atpB* as a control.

C. Chloroplast transcriptional activity

Cells were permeabilized through one freeze-thaw cycle, and pulse-labeled with ^{32}P-UTP for 15 min. Radiolabelled RNA was isolated and hybridized to a filter bearing the indicated gene probes. The two spots for each probe contained 0.6 and 0.3 µg of DNA respectively (except for the short psaAexon1 probe for which there was a single 0.25 µg spot).

Figure 6. TAA1 is required for translation of *psaA* mRNA

A. Expression of *psaA* mRNA

The levels of the *psaA* mRNA were determined by qRT-PCR from the *taa1* mutant strain, the *taa1* mutant strain harboring a poly(G) tract in the 5'UTR of intron-less *psaA* (*taa1/pG-psaA-Δi)*, the mutant strain complemented with *TAA1* and harboring the poly(G) tract in the 5'UTR of intron-less

psaA, (*taa1;TAA1/pG-psaA-Δi)* and the mutant strain transformed with an intron-less version of *psaA* as a control (*taa1/psaA-Δi)*.

B. Immunoblot analysis of PsaA

Total protein extracts from the same strains were subjected to SDS-PAGE and to immunoblotting with anti-sera against PsaA and CF_1 of ATP-synthase as a loading control.

Figure 7. Effect of iron limitation on the accumulation of TAA1, *psaA* mRNA and PsaA protein

A. Immunoblot analysis

Total protein extracts from two different WT strains, WT-8B and WT-137AH, and the *taa1* mutant strain complemented with the midigene carrying a triple HA epitope (*taa1*;*cw15*;*TAA1-HA)*, were separated by SDS-PAGE, and subjected to immunoblotting with anti-sera against TAA1 (or anti-HA monoclonal antibody in the case of *taa1*;*cw15*;*TAA1-HA)*, PsaA and CF_1 of ATP-synthase as a loading control. Cells from cultures in exponential phase were harvested and resuspended in TAP lacking iron (TAP-Fe), and the cultures were further diluted after 24h and 48h to maintain a low cell density. After 48h, Fe^{2+} was supplemented to the normal concentration of 18 µM. Samples were collected at the onset of the experiment (labelled +Fe), after 24h and 48h of iron deprivation (labelled -Fe 24h and -Fe 48h) and after 24h of recovery (labelled +Fe 24h).

B. Expression of *psaA* and TAA1 genes

The levels of the *psaA* and *TAA1* mRNA were determined by qRT-PCR on the same samples as in panel A from the WT-8B strain.

C. Stability of the TAA1 protein

Total protein extracts from the mutant strain complemented with the midigene carrying a triple HA epitope (*taa1*;*cw15*;*TAA1-HA)* were subjected to SDS-PAGE and immunoblotting with anti-HA monoclonal antibody or with anti-sera against CF_1 of ATP-synthase as a loading control. Cells from cultures in exponential phase were harvested and resuspended either in TAP with iron (+ Fe), or in TAP lacking iron (-Fe). After 2 hours, aliquots of the cultures were supplemented with cycloheximide (CHX), an inhibitor of cytosolic translation. Samples were collected at the onset of the experiment (labelled 0h), and after 6h in the different conditions.

For quantitation, lanes 1-4 show a dilution series (from 100% to 10%) of the sample in lane 1 (0h +Fe), supplemented with a wild-type extract (lacking TAA1-HA) to maintain a constant total amount of proteins.

Figure 1

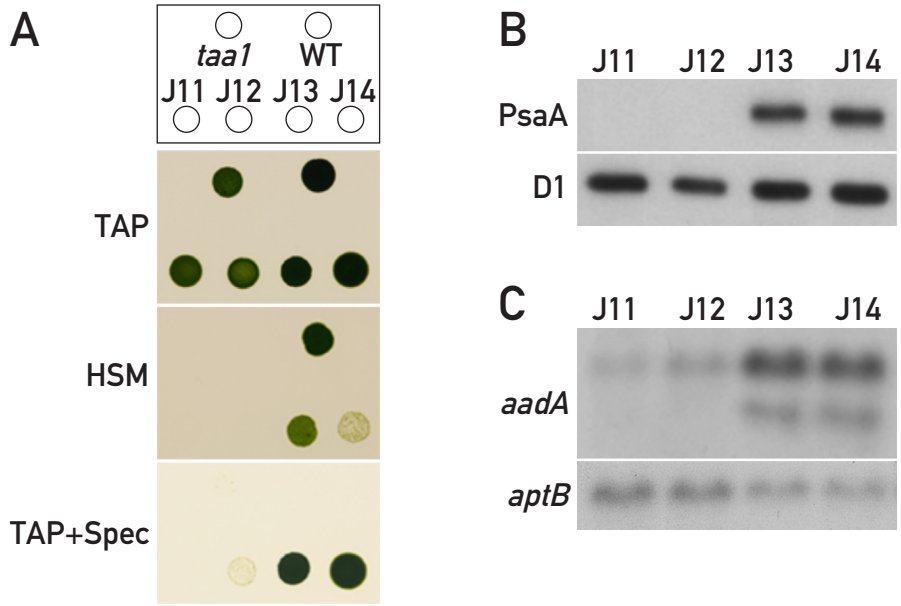

Figure 1. The 5'UTR of *psaA* is a genetic target of *TAA1*

A. Spot tests

Chlamydomonas cultures were spotted (10 µL) on minimal medium (HSM), on medium containing acetate (TAP) or on TAP medium supplemented with 100 µg mL^{-1} spectinomycin (TAP+Spec) under normal light (60 µE m^{-2} s^{-1}). J11 to J14 are the progeny of a tetrad from the cross *psaA*::*aadA;mt(+)* x *taa1;mt(-)*. The *psaA*::*aadA;mt+* strain is a chloroplast transformant with the *aadA* gene (conferring resistance to spectinomycin) under the control of the promoter/5' UTR of *psaA*. Wild-type (WT) and *taa1* strains are shown as controls.

B. Immunoblot analysis of PsaA

Total protein extracts from the progeny of the same tetrad were subjected to SDS-PAGE and immunoblotting with anti-sera against PsaA or the D1 protein of photosystem II as a loading control. The algae were grown in medium containing acetate (TAP) in the dark.

C. RNA-blot analysis of *psaA* mRNA

Total RNA extracts from the progeny of the same tetrad were subjected to denaturing agarose gel electrophoresis, blotted to Nylon membranes and hybridized with probes against *aadA* or *atpB* as a control. The nature of the lower band which is routinely observed for *aadA* is not known (Goldschmidt-Clermont, 1991).

Figure 2

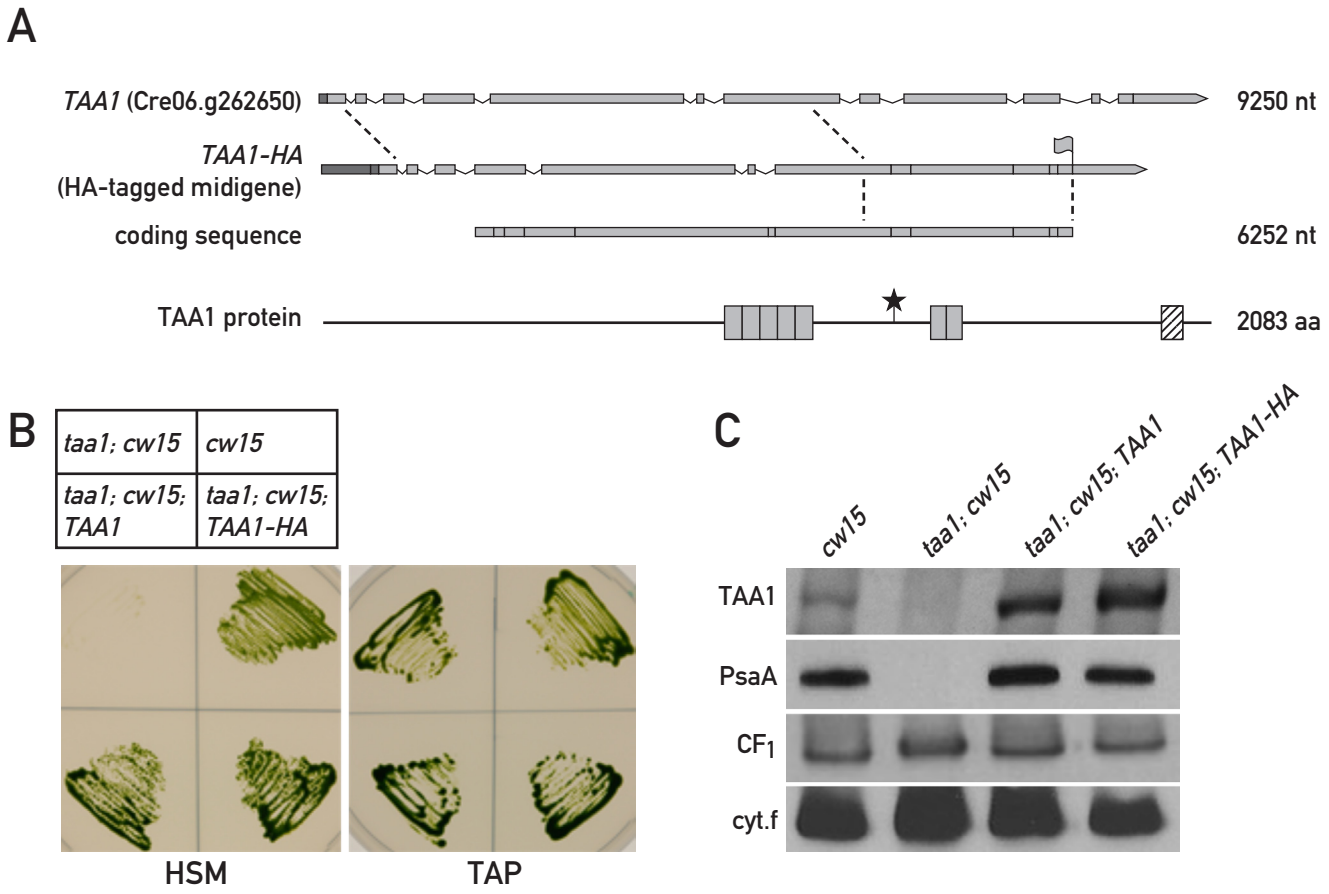

Figure 2. Characterization of the *TAA1* gene

A. Map of the *TAA1* gene

The first line is a schematic representation of the structure of the *TAA1* gene. The predicted pre-mRNA is 9'250 bp long, with a 5'UTR of 88 bp and a 3'UTR of 770 bp. The second line represents the structure of the midigene constructs with exons depicted as light grey boxes and the promoter / 5'UTR in dark gray. The 5' part of the genomic DNA is fused to the 3'part of the cDNA as shown with dotted lines. The flag represents the position of the triple HA epitope tag in pL37. The third line shows the exon structure of the coding sequence of *TAA1*. The bottom line depicts the structure of the TAA1 protein with the 7 OPR motifs shown as grey boxes and the RAP domain as hatched box. The star indicates the location of the premature stop codon in the *taa1* mutant.

B. Growth phenotype

Comparison of growth on minimal medium (HSM) and on medium containing acetate (TAP) under normal light (60 µE m^{-2} s^{-1}) of the mutant strain *taa1;cw15*, the control strain *cw15* and the complemented strains *taa1*;*cw15*;*TAA1* (transformed with the midigene pL30) and *taa1*;*cw15*;*TAA1-HA* (transformed with the midigene carrying a triple HA epitope, pL37).

C. Immunoblot analysis

Total protein extracts from the same strains were subjected to SDS-PAGE and immunoblotting with anti-sera against TAA1, PsaA, the CF_1 component of ATP synthase, and cytochrome f. The algae were grown in medium containing acetate (TAP) in the dark.

Figure 3

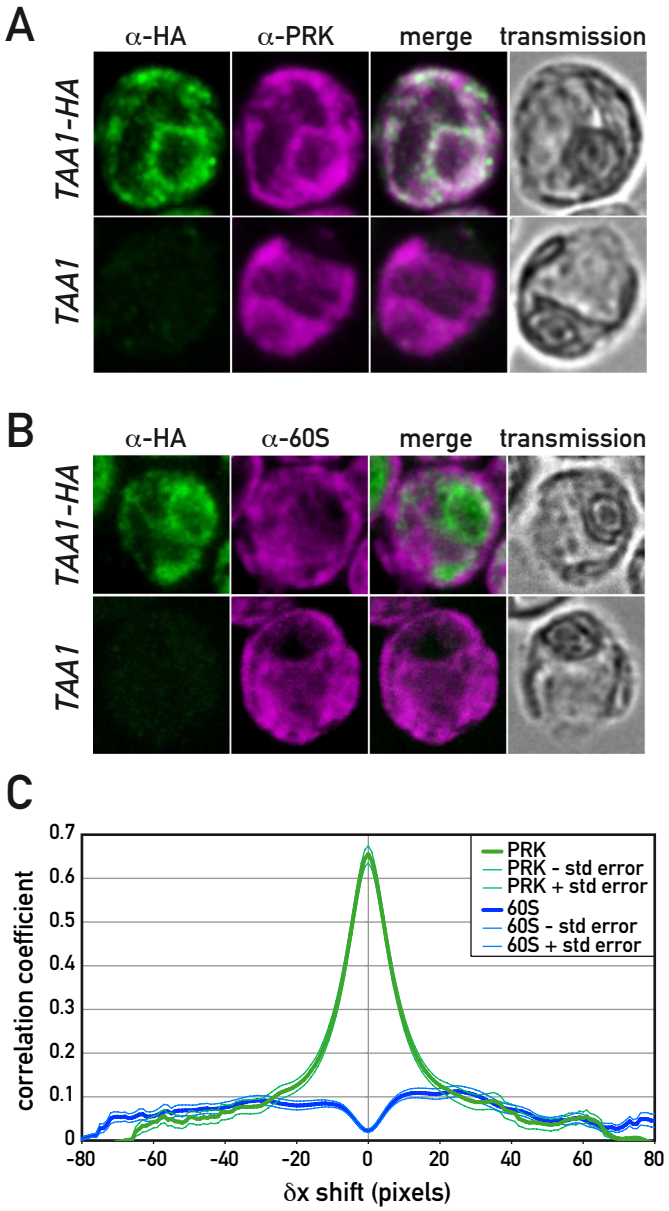

Figure 3. TAA1 is located in the chloroplast

A. Immuno-fluorescence of TAA1-HA in comparison to chloroplastic PRK

The first line represents staining in the *taa1* mutant strain complemented with the midigene carrying the triple HA epitope, *taa1*;*cw15*;*TAA1-HA*. The second line represents as a control the staining in the complemented strain with the midigene, *taa1*;*cw15*;*TAA1*.

B. Immuno-fluorescence staining pattern of the TAA1-HA protein in comparison to the cytosolic 60S ribosome subunit

The first line represents the staining in the *taa1*;*cw15*;*TAA1-HA* strain. The second line represents as a control the staining in the *taa1*;*cw15*;*TAA1* strain.

C. Quantitative analysis of co-localization

Van Steensel's analysis was applied to the co-stainings of TAA1-HA and PRK (green curves; average (thick line) ± standard error (thin lines) of n=43 cells) and of TAA1-HA and the ribosomal 60S subunit (blue curves; n=53 cells). This analysis consists in measuring Pearson's correlation coefficient between two fluorescent channels of a given image, and to plot the different values of this coefficient as one channel is shifted in x pixel by pixel relative to the other (see for review (Bolte and Cordelieres, 2006)). A peak at the δx=0 position indicates co-localisation of the two proteins studied (green curve: TAA1-HA and PRK); conversely, a local minimum at the δx=0 position indicates that the two signals are complementary (blue curve: TAA1-HA and the 60S ribosome subunit).

Figure 4

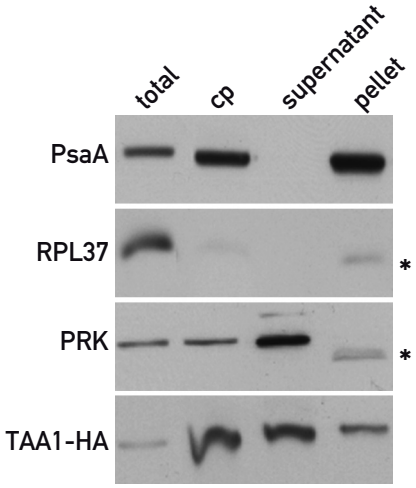

Figure 4. TAA1 is a partially soluble protein of the chloroplast

Fractions were prepared from the strain *taa1*;*cw15*;*TAA1-HA*. The four lanes contain total cell extracts (Total), the chloroplast fraction (Cp) and a chloroplast lysate fractionated by centrifugation into a soluble fraction (Supernatant) and a crude membrane fraction (Pellet). Equal amounts of protein (40µg) were loaded. Immunoblots were performed with antibodies against the HA epitope, PsaA (an integral membrane protein of Photosystem I), the cytosolic ribosomal protein RPL37 and PRK, a soluble chloroplastic protein. The bands marked with a star represent non-specific signals.

Figure 5

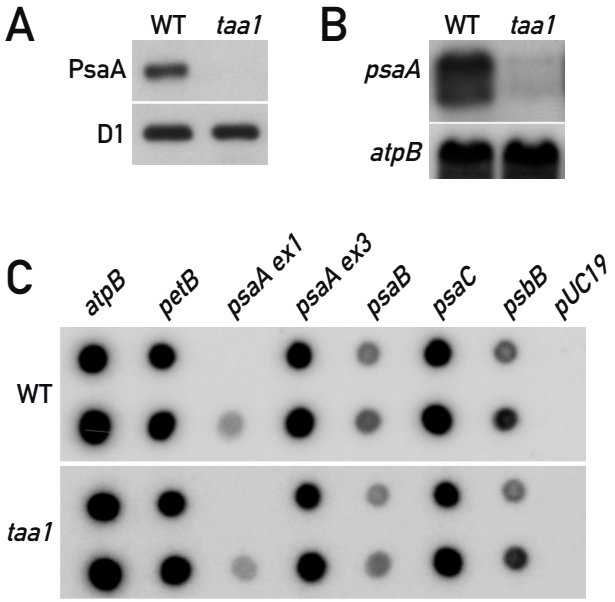

Figure 5. Stability of *psaA* mRNA is impaired in the *taa1* mutant

A. Immunoblot analysis of PsaA

Total protein extracts were subjected to SDS-PAGE and immunoblotting with anti-sera against PsaA and the D1 protein of photosystem II as a loading control. The algae were grown in medium containing acetate (TAP) in the dark.

B. RNA-blot analysis of *psaA* mRNA

Total RNA extracts from the same strains were subjected to denaturing agarose gel electrophoresis, blotted to Nylon membranes and hybridized with radiolabelled probes for exon 3 of *psaA*, or *atpB* as a control.

C. Chloroplast transcriptional activity

Cells were permeabilized through one freeze-thaw cycle, and pulse-labeled with ^{32}P-UTP for 15 min. Radiolabelled RNA was isolated and hybridized to a filter bearing the indicated gene probes. The two spots for each probe contained 0.6 and 0.3 µg of DNA respectively (except for the short psaAexon1 probe for which there was a single 0.25 µg spot).

Figure 6

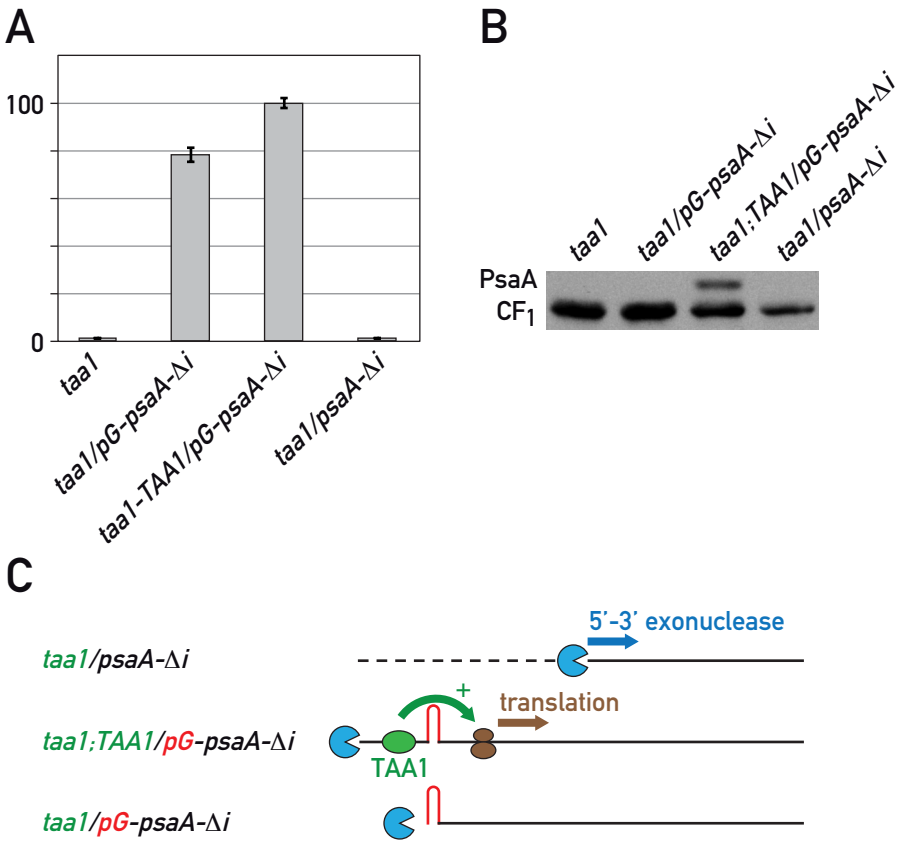

Figure 6. TAA1 is required for translation of *psaA* mRNA

A. Expression of *psaA* mRNA

The levels of the *psaA* mRNA were determined by qRT-PCR from the *taa1* mutant strain, the *taa1* mutant strain harboring a poly(G) tract in the 5'UTR of intron-less *psaA* (*taa1/pG-psaA-Δi)*, the mutant strain complemented with *TAA1* and harboring the poly(G) tract in the 5'UTR of intron-less *psaA*, (*taa1;TAA1/pG-psaA-Δi)* and the mutant strain transformed with an intron-less version of *psaA* as a control (*taa1/psaA-Δi)*.

B. Immunoblot analysis of PsaA

Total protein extracts from the same strains were subjected to SDS-PAGE and to immunoblotting with anti-sera against PsaA and CF_1 of ATP-synthase as a loading control.

Figure 7

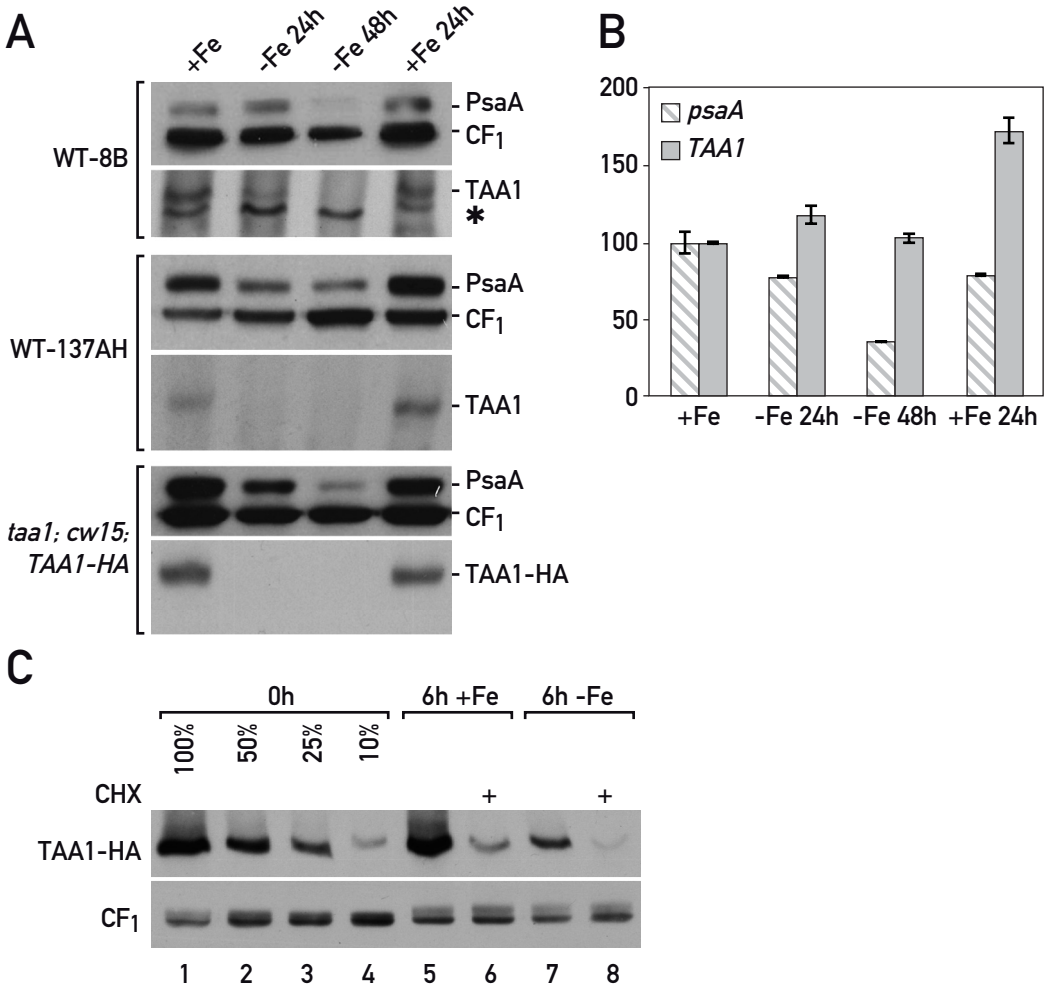

Figure 7. Effect of iron limitation on the accumulation of TAA1, *psaA* mRNA and PsaA protein

A. Immunoblot analysis

Total protein extracts from two different WT strains, WT-8B and WT-137AH, and the *taa1* mutant strain complemented with the midigene carrying a triple HA epitope (*taa1*;*cw15*;*TAA1-HA)*, were separated by SDS-PAGE, and subjected to immunoblotting with anti-sera against TAA1 (or anti-HA monoclonal antibody in the case of *taa1*;*cw15*;*TAA1-HA)*, PsaA and CF_1 of ATP-synthase as a loading control. Cells from cultures in exponential phase were harvested and resuspended in TAP lacking iron (TAP-Fe), and the cultures were further diluted after 24h and 48h to maintain a low cell density. After 48h, Fe^{2+} was supplemented to the normal concentration of 18 µM. Samples were collected at the onset of the experiment (labelled +Fe), after 24h and 48h of iron deprivation (labelled -Fe 24h and -Fe 48h) and after 24h of recovery (labelled +Fe 24h).

B. Expression of *psaA* and TAA1 genes

The levels of the *psaA* and *TAA1* mRNA were determined by qRT-PCR on the same samples as in panel A from the WT-8B strain.

C. Stability of the TAA1 protein

Total protein extracts from the mutant strain complemented with the midigene carrying a triple HA epitope (*taa1*;*cw15*;*TAA1-HA)* were subjected to SDS-PAGE and immunoblotting with anti-HA monoclonal antibody or with anti-sera against CF_1 of ATP-synthase as a loading control. Cells from cultures in exponential phase were harvested and resuspended either in TAP with iron (+ Fe), or in TAP lacking iron (-Fe). After 2 hours, aliquots of the cultures were supplemented with cycloheximide (CHX), an inhibitor of cytosolic translation. Samples were collected at the onset of the experiment (labelled 0h), and after 6h in the different conditions.

For quantitation, lanes 1-4 show a dilution series (from 100% to 10%) of the sample in lane 1 (0h +Fe), supplemented with a wild-type extract (lacking TAA1-HA) to maintain a constant total amount of proteins.

A nucleus-encoded helical-repeat protein which is regulated by iron availability controls chloroplast *psaA* mRNA expression in Chlamydomonas

Linnka Lefebvre-Legendre, Yves Choquet, Richard Kuras, Sylvain Loubéry, Damien Douchi and Michel Goldschmidt-Clermont.

SUPPLEMENTAL DATA

Supplementary Figure 1. Structure of the TAA1 protein

Amino-acid sequences of the TAA1 protein, the OPR motifs and the RAP domain. The OPR motifs are highlighted in blue and pink and the RAP domain in green. The consensus sequence derived from the 7 OPR repeats was determined using WebLogo (Crooks et al., 2004).

Supplementary Figure 2. Genotyping of the *taa1/pG-psaA-Δi* chloroplast transformant

A schematic representation of the transformed loci is shown at the top (dark blue lines represent the flanking sequences that were present in the transformation vectors).

Homoplasmicity of the chloroplast insertion was determined by PCR on total DNA extracts(Lefebvre-Legendre et al., 2014). The absence of the parental genome (where *psaA* exon3 is flanked by the 3'part of split intron 2 (3' i2) rather than exon2) is revealed by PCR1 which gives a PCR product of 290 bp with WT DNA and 850 bp with transformed DNA. The presence of the intron-less *psaA* gene carrying the polyG tract is revealed by PCR2 which gives a PCR product of 1000 bp consisting of exon 1, exon 2 and a part of exon 3.

PCR on total DNA extracts (Cao et al., 2009) used the following protocol: 5 min at 95 °C / 40 cycles [1 min at 95 °C, 1 min at 54°C or 60 °C (depending on the Tm of the primers) , 1 min at 72 °C] / 7 °C.

PCR1: primers psaAfor1 and psaArev1 (Tm=54°C) (see Supplementary Table 1)

PCR2: primers psaA- ex3-5'UTR for and psaA-ex3-rev (Tm=60°C)

SUPPLEMENTARY TABLES

Supplementary Table 1. Rescue of taa1 by transformation with TAA1 constructs.

The *taa1;cw15* mutant was transformed in duplicates using the glass-bead transformation method (Kindle, 1990) with the plasmids listed in the left column.

Transformation with:	**# of colonies**	
No DNA control	0	0
64B4 (TAA1 cosmid)	18	30
64B4E (EcoRI fragment of 64B4)	44	41
pL30 (TAA1 midigene)	40	48
pL37 (TAA1 midigene with HA epitope tag)	34	40
pL57 (TAA1 midigene with C-terminal deletion)	0	0

Supplementary Table 2. Oligonucleotides used in this work

psaAfor1	ATGACAATTAGTACTCCAGAGCG
psaArev1	ACCAACGTGACCTTCACC
psaA ex3 5'UTR for	GTGAAAATTGCATGCACGGCTCTTAAG
psaA ex3 rev	GGAGCAGCTTTGTGGTAGTGGAAC
BspEI For	GCTCCGGAGGCGCGCGG
Stop rev	CTCAAGGCCTCTGCGGCTGCGAC
NsiI Rev	AGATGCATCCCAAACTTGCTGCAcagg
Stop For	GCAGaggcctTGAGGGGCTGGC
E9 down	GCTCCAGAGCCAGCAGCCGAGG
5103 up	GCGGTCCCGACTCCCGCAA
E9 up	CCTCGGCTGCTGGCTCTGGAGC
E11 down	CGTCATGGCGAGCGTTACACGTACG
6541up	GTGCTGAGCGACAGGGCTGCTTC
3531 up	CTAGGGCTGCTGGAGCAGCGG
4012 down	GCCTCAGTCGCGTCTGCCTCCA
4012 up	TGGAGGCAGACGCGACTGAGGC
5103 down	TTGCGGGAGTCGGGACCGC
qPCR psaAEx1 For	AATGGGCTAAACCAGGACATTTTTCAC
qPCR psaAEx3 Rev1	CATGGAAGTACATACCACTTAACCAAATGAAAATGA
qRT TAA1 Fw1	CGACAGCAACTGTTTCGCGATG
qRT TAA1 Rv1	GACCTGCGTCTGTTGTTGCTTTG
qRT RPL13 For1	ATTCTTGCCGGGCAGCAGATTGTG
qRT RPL13 Rev1	TTGCGCAGGAAGCGGTCATACTTC
qUBQ2 For	GCGATTTCTCGTTGGGCAGT
qUBQ2 rev	TGGCCCATCCACTTGTCCTT
Ab-F23-2 For	GGATCCCCCAGTCGCGCGG
Ab F23-2 Rev	CTCGAGTCAGGACGGCGTGCTG

Supplementary Figure 1

MQSHCAHYKAGAAARREKSSREISSSAPTRPLHCRSSQPSRAITFAINLRADGSYDAGLT
RPQAARQRARRRTGPPSTATVSRWSASDSDASRFDWLDGAKQQQTQVLVDALFAAESVPP
PRLPVLLALLEGRPDLEQALVEAGLPAAAAAVLRSDLLQRLLPGGLLLETLMGLIEDRAT
ELPAEQLLMACRLVAAWHPPNGCEALGPASASLATAIADAVLAGPDSTGEADKADSRGSG
GSSADFAATAGMLADALTLLQPWLAWRASGSGSAAAAAGTSAASAAALGLLDAGVAAAEE
AAEAADALAAARGAAEALLRRPEVAAAADTGVLLAVTAAAAAYDVEVPRDLARTAVSLAS
TASSSSPTASAGSSSTTSSGAGSSSATTAAELAAQLVAASVAGAAGGAAGHGRGRGRNQL
SGEELESVVWARLASEVGAAEHAAFLRELLGRVRQMAPGSGRLQLQPEEQQHEQQPGSKA
GEAGPADEQQAARRALVVALGSAAGGLGPDALALAAECAAAVFPGDTIGDGADALASTAA
AELLGCAADASAEPAAACTADQVCRLAAAVLALRARVGASVNETAVARVLAAAEAVQLQS
ASTDAVAALVAAAAVPGGGLALPPPLVDALLVQLTAAAATAAPVEDVAVDGSAGTAKSGR
KQEAAPAAAAVAQLTPQQAAALLEVAVAAAEEAAQAAAAAVPSSSTAAEPATPAPIPPQR
AAVLCAAIDVAMRLLTPSVRRVDSVSDITRLLVLAHRCQRAGLRPREQRGLLWAAHERLR
VLGLSMSPAEAVGVLRACAALKWAPSVLFSELLLPLLRQLQASAAAAAAAAGGPSPASGA
GSTSGADDTSALGAWGEAGSGGAASRPWTLREVRSALALLAAVGYDGPMAASLVKLGVGE
LLRAHHVAATAASRRSSSEAGAEGEGALLGAEDMTQLLWVCVALRYRGGAVLRPLLQLLL
LVPAPQVSVRAAAQAVWAAARLGVVGERLVRWALAACQGQGKLAAAPPQSLANLCWGLGK
LGVKPPRAFVTAMAVASLGQLPHFTPQELATTAFVLATWGGRLGAAASGLVRHVVATRSH
FDGPALCVAAWAVQRLAAAPPADATADAAASADVTPGLDAASLGLLEQRLLEAVQEAAHE
RRGRPGTGDFLQSLPGVADHHLLRFFSAASAAGYRPAALLAAYCDALLPRLQRFNGCSPA
AAAGAARRARLLWSAARVLQTFRVTAAERPELLAALEHAAEQCQAILGPQALAGVLSAMS
DLGHYPAGWAARGLLRCVRLGLVEADATEAAAIVAALAAWGERLEEGEAAAAAAAAAAAA
GAEDGRQGNGLAAAGGEEAGNPSRAAKAAKPAPSGKQAVSRRLDLLRQVAVARLTELCVP
PPVVAAAGPGAAAAAAAHGQALPSAAGAAAAAPSPAEASGAGLTPAAAATAAAAAEAPSA
GGAIAQPSIEPEVALSLLRSLARLRWHSDPLEGALVRAAAALTADPAGRRRVPALTTLLW
AMASLRQDVPELLDDLQAALMGLPRNTRSLAEEVALLESGRLAGALGADSQRPPAPPSVP
PVQPVQPVQQHSQAAAEPTPVVEASAQPTVVLAAAQAAAQPRPSPAASPSAPSTPSNSTT
ASAAASNNHNHNSTNGNGLLARPNKPAVPTPATADTVSPTASLSSLSSLSSMDGGAGGGF
DTAAATAAAAAALNQRLEQQLVGAAGRGRLASEPWAPVDVFKALWACAKMNRHPGPQILA
AAERSWVLHTTDGAAGGAEGRTLPPLHTVTGLLWSLSVFRHHNSAFAQQLAAQLAARLGV
LAAAAAADGGEADGAAAAAAALEKQAPQLAACLLAAAADRTDSPLNAALAPEARGRLLNV
WRARQAERVARPPGRYQTDLVSVLRKMGYTAAANVATPDGVAVADVAVAVTPNAGLRAAS
TASASPGTSSTSSMDSGDGAAAATAATADSGLGSGAAAAAAAAPAPAAPRLLALELVGRH
NSAANSPRIMGEAVIKYRLLQAHGYLVVPVSCYEWDRISHQDVWTKMVYLQAKIDRRTGT
GLAASSVSAAAAAAAAAPAAGAEGQTQTQAVSASSGLSRSQPQ

OPR

928	964	LLGAEDMTQLLWVCVALRYRGGAVLRPLLQLLLLVPA
966	1002	QVSVRAAAQAVWAAARLGVVGERLVRWALAACQGQGK
1005	1042	AAPPQSLANLCWGLGKLGVkPPRAFVTAMAVASLGQLP
1043	1079	HFTPQELATTAFVLATWGGRLGAAASGLVRHVVATRS
1080	1117	HFDGPALCVAAWAVQRLAAaPPADATADAAASADVTPG
1448	1484	SIEPEVALSLLRSLARLRWHSDPLEGALVRAAAALTA
1489	1525	RRRVPALTTLLWAMASLRQDVPELLDDLQAALMGLPR

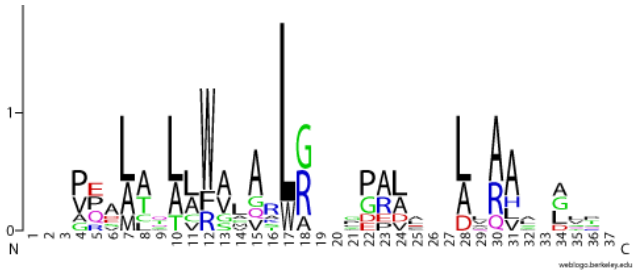

RAP

1978	2031	GRHNSAANSPRIMGEAVIKYRLLQAHGYLVVPVSCYEWDRISHQDVWTKMVYLQ

Supplementary Figure 1. Structure of TAA1 protein

Amino-acid sequences of the TAA1 protein, the OPR motifs and the RAP domain. The OPR motifs are highlighted in blue and pink and the RAP domain in green. The consensus sequence derived from the 7 OPR repeats was determined using WebLogo (Crooks et al., 2004).

Supplementary figure 2

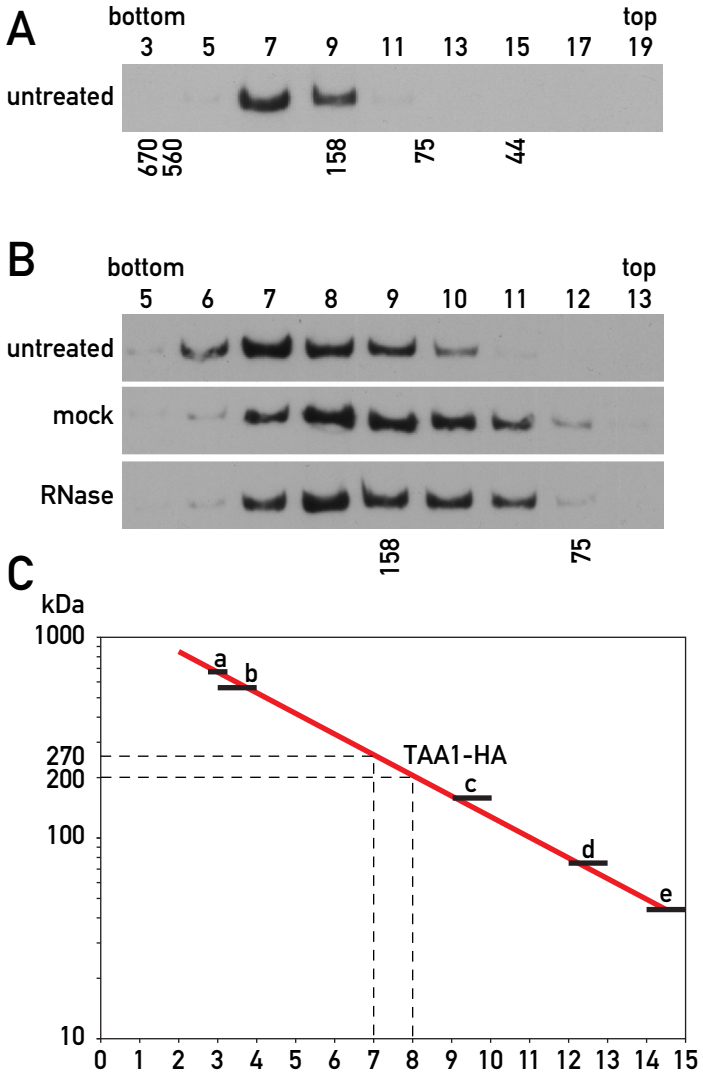

Supplementary Figure 2. Sucrose gradient sedimentation analysis of TAA1 complexes.

Total soluble proteins from the *taa1; TAA1-HA* strain were fractionated by sedimentation in sucrose density gradients. Prior to sedimentation analysis, on aliquot was kept on ice (untreated), while two other aliquots were either supplemented with RNase (RNase) or with buffer (mock) and incubated for 10 minutes at 22 °C. For calibration, a parallel gradient was loaded with protein markers. A total of 22 fractions were collected from the bottom of each tube.

A. Alternate fractions (fraction 3 to fraction 19) were analyzed by SDS-PAGE and immunoblotting with anti-HA serum. The migration of the markers is indicated with the corresponding molecular masses at the bottom of the panel

B. All fractions in the region of the gradient containing TAA1-HA (fractions 5 – 13) were analyzed as in A.

C. Calibration. A semi-logarithmic plot of the molecular masses of the markers against the fraction(s) to which they migrated is shown. The migration of TAA1-HA in the untreated sample (fraction 8) and in the RNase-treated sample (fraction 7) is shown with dotted lines, corresponding to apparent molecular masses of 200 kDa and 270 kDa respectively.

a: 670 kDa	Thyroglobulin
b: 560 kDa	RubisCO as determined by reprobing the membrane shown in A
c: 158 kDa	Aldolase
d: 75 kDa	Conalbumin
e: 44 kDa	Ovalbumin

Supplementary Figure 3

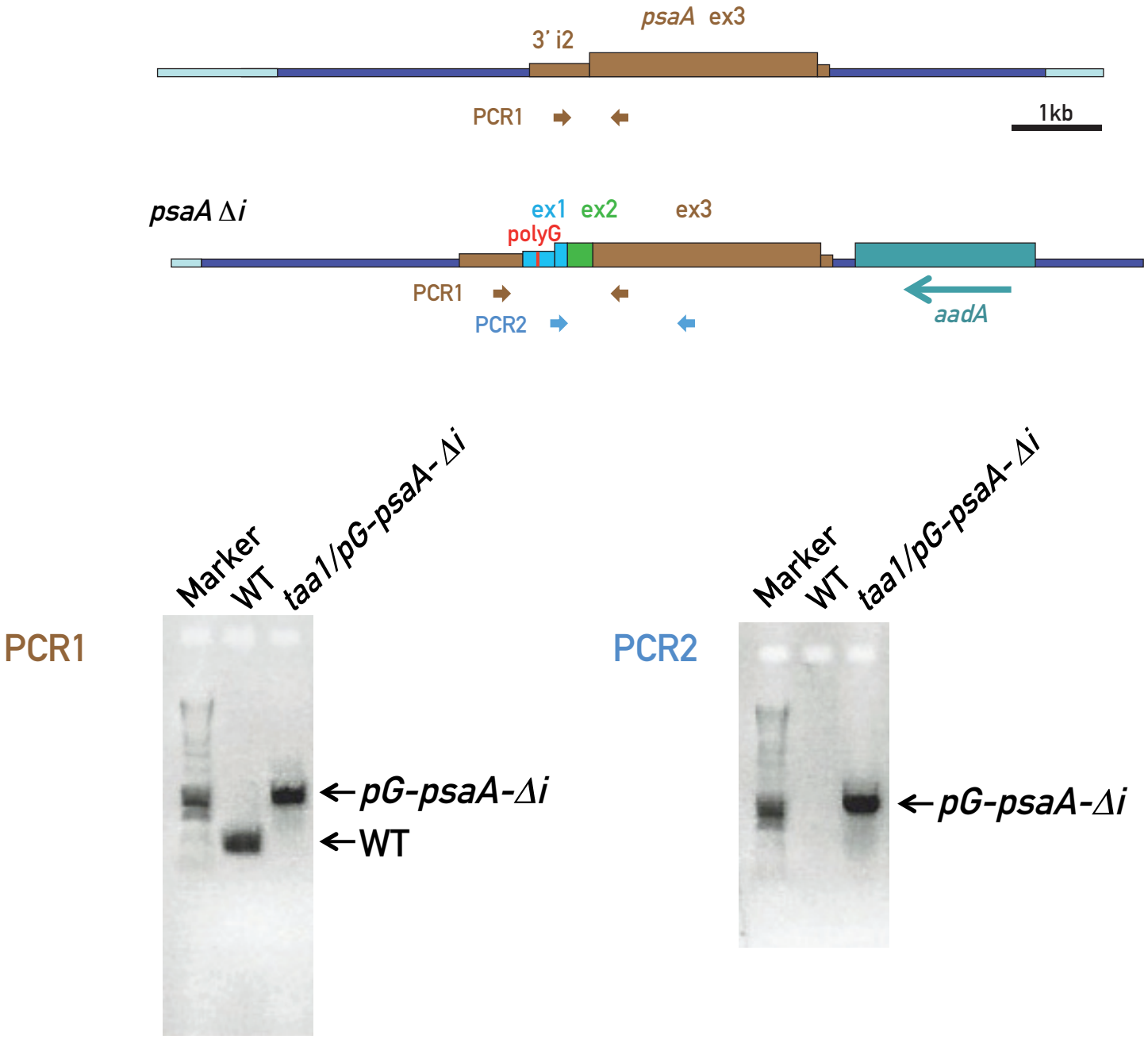

Supplementary Figure 3. Genotyping of the *taa1/pG-psaA-Δi* chloroplast transformant

A schematic representation of the transformed loci is shown at the top (dark blue lines represent the flanking sequences that were present in the transformation vectors).

Homoplasmicity of the chloroplast insertion was determined by PCR on total DNA extracts(Lefebvre-Legendre et al., 2014). The absence of the parental genome (where *psaA* exon3 is flanked by the 3'part of split intron 2 (3' i2) rather than exon2) is revealed by PCR1 which gives a PCR product of 290 bp with WT DNA and 850 bp with transformed DNA. The presence of the intron-less *psaA* gene carrying the polyG tract is revealed by PCR2 which gives a PCR product of 1000 bp consisting of exon 1, exon 2 and a part of exon 3.

PCR on total DNA extracts (Cao et al., 2009) used the following protocol: 5 min at 95 °C / 40 cycles [1 min at 95 °C, 1 min at 54°C or 60 °C (depending on the Tm of the primers) , 1 min at 72 °C] / 7 °C.

PCR1: primers psaAfor1 and psaArev1 (Tm=54°C) (see Supplementary Table 1)

PCR2: primers psaA- ex3-5'UTR for and psaA-ex3-rev (Tm=60°C)